People's Democratic Republic of Algeria
Ministry of Higher Education and Scientific Research

University M'Hamed BOUGARA – Boumerdes

Institute of Electrical and Electronic Engineering

Department of Power and Control

Final Year Project Report Presented in Partial Fulfilment of
the Requirements for the Degree of

MASTER

In **Power Engineering**

Option: **Power Engineering**

Title:

Phasor Measurement Unit Placement Optimization Based on Meta-heuristic Methods for Reliable Observability of Power System

Presented by:

- **KOUZOU Ahmed Lakhdar**

Supervisor:

Pr. BENTARZI Hamid

Registration Number:...../2019

Abstract

The phasor measurement units (PMUs) play an important and vital role in power system monitoring and control, they provide power system phasors stamped with a common real time through a global positioning system (GPS). From economical point of view, it is not possible to install PMUs in all system buses due to the high cost and the requirement of more complex communication systems. Therefore, an optimal PMUs placement (OPP) problem is formulated to minimize such requirements. In this context, the main aim of the present project is to use an optimal approach to select the minimum number of PMUs location using meta-heuristic algorithms. The simulation of the used approach has been performed and tested on selected power systems using MATLAB software.

Key-words: PMU, OPP, Meta-heuristic Methods.

Dedication

I have a great pleasure to dedicate this modest work

To my Beloved Mother and my Dear Father

To my Dear Sister, Brothers, Uncles, Aunts and Cousins,

Specially Maria

To all my Friends, Specially Youcef

To all my Teachers from my first year of primary school to my last year of university

KOUZOU Ahmed Lakhdar

Acknowledgement

First and foremost, we are thankful to Allah, the most gracious, the most merciful for helping me finish this modest work. It is my belief in him that helped me persevere at times when it seemed impossible to go on.

Thanks to my beloved parents who have pushed me to overpass all obstacles and hitches I faced in my entire life, their love and guidance are with me in whatever I pursue.

I would like to express my sincere gratitude to my supervisor ***Pr. BENTARZI HAMID*** *who accepted to supervise me for the present work and for his help and patient during the preparation of this Project.*

A special thanks to Dr. Mohammedi R.D and Dr. Laouamer M for their precious help during this project.

My deepest gratitude goes to my grandmothers, my grandfather souls, all my family for their unflagging love and support throughout my life and studies.

Finally, a special thanks go to all IEEE members.

KOUZOU Ahmed Lakhdar

Table of Contents

List of Tables

List of Figures

List of Abbreviations and Acronyms

ADC	Analog to digital converter
CS	Cuckoo search
CT	Current transformer
DFT	Discreet Fourier transform
EMS	Energy management system
FIDVR	Fault-induced delayed voltage recovery
FFT	Fast Fourier transform
GPS	Global positioning system
GWO	Grey wolf optimizer
IPSO	Improved particle swarm optimization
KCL	Kirchoff's current law
KVL	Kirchoff's voltage law
MFO	Moth-flame optimization
OPP	Optimal PMU placement
OPPP	Optimal PMU placement problem
PDC	Phasor data concentrator
PMU	Phasor measurement unit
PPS	Pulse per second
PSO	Particle swarm optimization
PT	Potential transformer
ROCOF	Rate of change of frequency
SCADA	Supervisory control and data acquisition
SCDR	Symmetrical component distance relay
SE	State estimation
SOC	Second of century
SORI	system observability redundancy index
TVE	Total vector error
WAMS	Wide area measurement system
WDO	Wind driven optimization
ZIB	Zero injection buss

General Introduction

The electrical power system is the more crucial system developed for ensuring the supplying of electrical energy over the entire world and in the same time it is considered to be one among the most complex systems. However, failures occur frequently in this system and they can cause great trouble to the humanity at all levels from domestic application to industrial application and other vital applications, which are based on electrical energy. Therefore, the stability of this system is of great interest, where the absence of adequate actions for handling in real time the unexpected faults will lead to the blackout. Consequently, exorbitant economic losses at all levels and drastically human situation may be produced [1].

Indeed, the power system failures are caused by many factors like the subjection of the power transmission and distribution system to an overstressed conditions due to the continuous increase in electricity consumption and the inadequate observability of the system, which affect the control, the monitoring and the protection of the whole power systems [2]. Thus, the accurate monitoring of power system becomes the most important function for ensuring better controllability, higher reliability and stability of the power system. The classical monitoring system is performed based on the measurement collected from the supervisory control and data acquisition (SCADA) system. Indeed, the SCADA provides information to power dispatchers, system protection workers and maintenance substation workers….etc. The mechanism used in this system to collect the measurement is asynchronous and relatively slow, so the fast and dynamic phenomena cannot be captured efficiently as the case of the power network e.g. short-duration disturbances. Furthermore, the provided data does not include the accurate phase angle of bus voltages and line currents [3]. Nowadays, real-time measurements as well as voltage and current phasors can be supplied by Phasor Measurement Units (PMUs).

A PMU or Synchrophasor is a digital device which measures node voltage and branch current phasors in a power system with very high sampling rate and precision synchronized by a common timing signal from a global positioning satellite (GPS) clock [4].

The Phasor measurement units become popular due to their wide range of applications and benefits over the classical SCADA system [5]. In this project, a proposed optimal approach will be used to select the location where the PMUs to be installed with minimum number based on meta-heuristic algorithms. The main aim is to ensure the full observability. The simulation of the proposed methods will be performed and tested on selected power systems using MATLAB software. This project report is organized in four chapters as follows:

Chapter1- PMU state of art: A general overview about the PMU and its architecture.

Chapter 2- The PMU Optimal Placement Problem (OPPP) formulation.

Chapter 3-The selected Meta-heuristic Algorithms which will be used for solving the OPPP.

Chapter 4- Application of the selected optimization algorithm on solving the OPP problem of some selected power systems.

CHAPTER 1

PMU State of Art

- *Introduction*
- *Signal representation*
- *Phasor Measurement Unit technology*
- *Wide Area Measurement System (WAMS)*
- *Overview about Power System State Estimation*
- *The Comparisons between SCADA system and PMUs system*
- *PMU challenges*
- *Conclusion*

PMU State of Art

1.1 Introduction

The modern phasor measurement systems appeared as a result of the innovation and development of the Symmetrical Component Distance Relay (SCDR) in the early 1970s [6]. Indeed, the SCDR used the symmetrical components of voltages and currents, which are the backbone of most power system analysis programs such as load flow, short circuit, stability, state estimation, optimum power flow … etc. Whereas, efficient methods were utilized by the SCDR for measuring symmetrical components of voltages and currents, these efficient methods are proved to be very interesting for many applications [7]. In this context, many researchers have developed techniques, which determine the state of the power system in real time based on real time measurements. However, it was not possible at that time to ensure the synchronized measurements. After that, a technique has been developed to overcome this main problem and to enable obtaining the measurements by sequential scanning, and then the state of the power system has been estimated. This estimated state contained only the positive sequence voltages for all network buses [7].

On the early 1980s, the global positioning system (GPS) satellites have been deployed in significant numbers. Then, it was obvious that the use of the GPS time signals as inputs to the sampling clocks of the digital relay measuring system provides a very powerful measurement tool and an instantaneous image of the state of the power system. The GPS which has been invented and deployed by the U.S. Department of Defence has given birth to the next generation of phase measurement devices, which were called the Phasor Measurement Unit (PMU) [8]. Using the GPS transmissions the PMUs synchronize the sampling clocks to have a common reference for the calculated phasors across the power system. The PMU were first developed in the Power System Research Laboratory of Virginia Tech, the model of this PMU is depicted in Figure 1.1.

After this work, a lot of demo projects were developed, focusing on the PMU applications, the GPS receivers of satellite systems were very expensive at that time due to the precise of the internal crystal clocks that keeps time accurate until the next GPS satellite came into view.

Nowadays, as a result of the fully development and deployment of the satellite system the GPS receiver chip set could be obtained by just a few hundred of dollars. In addition to that, the number of manufacturers grew up to tens of producers now. Users can achieve 24-hour continuous information processing in real time that is synchronized with the international

standard time UTC. Furthermore, a high precision timing is obtained by the GPS system, this precision is ranging from 1 to 10 ns [10]. Simultaneously, in one second interval the GPS receiver can deliver a unique pulse signal known by one pulse per second (PPS). Thus by installing or embedding GPS receivers into different devices, the unsynchronized standard time problem of power system will be resolved.

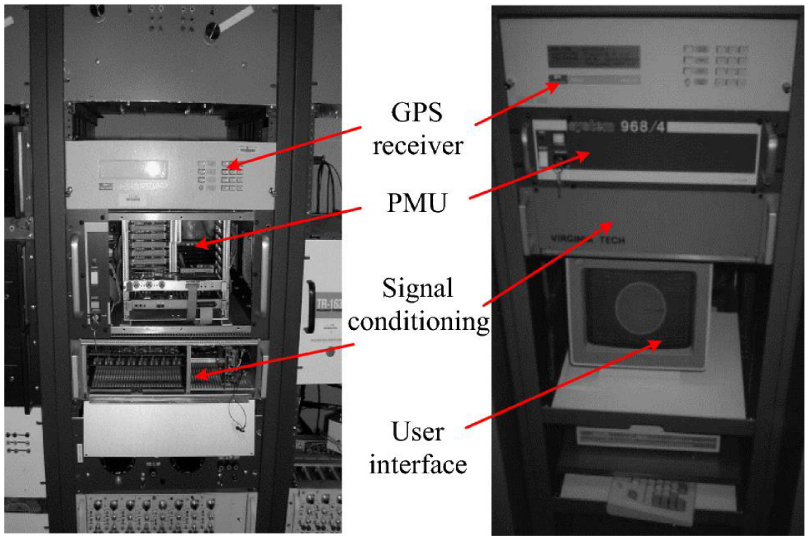

Figure 1.1. *First set of PMUs built at Virginia Tech in 1980s [9]*

The IEEE began a long and complex standardization process. The first version of the PMU standard was published in 1995. The work has been revised further up to the latest 2018 release (IEC/IEEE 60255-118-1).

1.2 Signal representation

The world around us has different measurable quantities. Some quantities are constant like acceleration due to gravity, speed of light…etc. Some are time-varying like AC voltage, temperature…etc. It means that as time goes on, they change their values. By other words, signal means simply any quantity values taken over a period of time.

Both of voltage and current in power system are alternating, An alternating function or AC waveform is defined as one that varies in both magnitude and direction with respect to time, by other words it is a time-varying waveform. The shape obtained by plotting the instantaneous coordinate values of either voltage or current against time usually modelled as a function including either the cosine or the sine trigonometric identity. However, transforming it into the frequency plane is often more appropriate, both for understanding and for simplifying the equations.

1.2.1 Sinusoidal signal representation

The voltages and currents in the time domain are usually described as sinusoidal signals, they can be mathematically modelled using trigonometric identity as follows:

$$f(t) = Acos(\omega t + \emptyset) \ \ or \ \ f(t) = Asin(\omega t + \emptyset) \tag{1.1}$$

Where $\omega = 2\pi f$

The signal gives the values of the considered quantity at different values of time. The maximum value of the sinusoidal signal is also called its amplitude (A) where (2A) is pick to pick magnitude. Here ω is called angular frequency of the signal, its unity is (rad/s) which in power systems is defined as $2\pi f$ with f is being the frequency of the system measured in Hertz (Hz). $\emptyset$ is called the phase angle or phase difference measured in Radians (rad). The phase angle differs according to the reference.

In our home and industries, all the power signals are AC sinusoidal signals. The frequency in Algeria and in almost the world countries is 50 Hz where such frequency in USA is 60 Hz.

1.2.2 Phasor representation of sinusoids

In Electrical Engineering, the phasor of a voltage/current signal is a fundamental concept. A pure sinusoidal waveform of a magnitude and a phase with respect to a reference can be represented by a unique complex number known as a phasor. Consider the following sinusoidal signal:

$$x(t) = X_p cos(\omega t + \emptyset) \tag{1.2}$$

The phasor representation of $x(t)$ can be written as follows:

$$X = \frac{X_p}{\sqrt{2}} e^{j\emptyset} = \frac{X_p}{\sqrt{2}} \big(cos(\emptyset) + jsin(\emptyset)\big) \tag{1.3}$$

The magnitude value of the phasor is $\frac{X_p}{\sqrt{2}}$ which presents exactly the root mean square (RMS) value of the given sinusoid $x(t)$. In addition, the frequency of the signal is not explicitly stated in the phasor representation, it is clear that all phasors in one phasor diagram must be of the same frequency. A sinusoid and its representation as a phasor are illustrated in Figure 1.2. Whereas, the phase angle of the phasor depends upon the choice of the reference axis.

It is mentioned previously that only the pure sinusoid can be represented by a phasor representation. Practically, any signal has noises of different other frequencies, then it is necessary to extract a single frequency component of the signal (frequency of interest) to be represented as a phasor which corresponds to the fundament direct component of the considered signal. Techniques based on the “Fourier Transform” are often used to decompose

a signal into many signals with different frequencies, and also to extract the single signal with the frequency of interest. In digital or sampled data system the discreet Fourier Transform DFT or the Fast Fourier Transform FFT will be used. Also according to the phasor definition the sinusoid should be permanently unchanged, that is why in practise the phasor representation is considered for a portion of time span which is known as data window and it is a very important parameter in phasor estimation of practical waveforms [11].

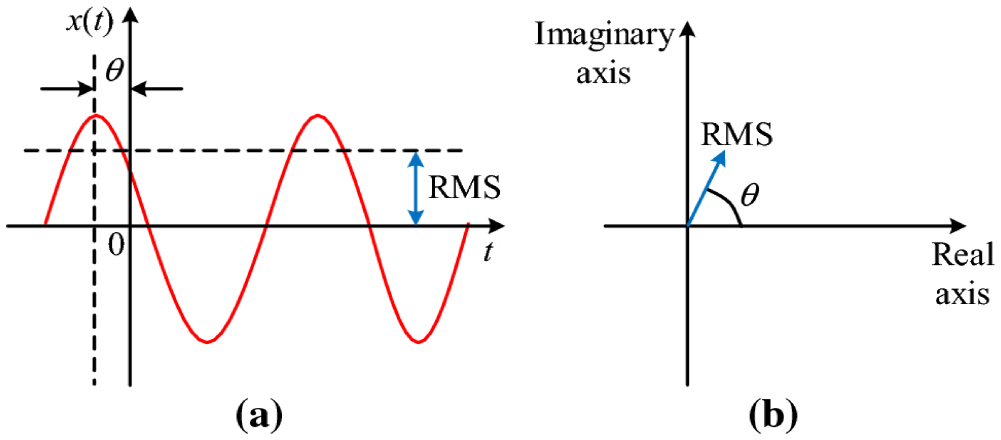

Figure 1.2. *A sinusoid (a) and its representation as a phasor (b) [9]*

1.3 Phasor Measurement Unit technology

Today, Phasor technology is considered to be one of the most important measurement technologies of power systems because of its unique ability of sampling analog voltage and current waveforms data in synchronism using a GPS clock and calculate the corresponding 50/60 Hz phasor component. In all different location of power system, this synchronized sampling process provides a common reference for the phasor calculations.

1.3.1 What is a PMU?

The PMUs are devices, which are used for monitoring the power system that have traditionally been designed to provide a scalar information. These devices provide voltage and current phasors as RMS values stamped with time.

Due to the transition from analog and electromechanical devices to digital devices, a great evolution have been made in this field. This digital devices have enabled more sophisticated measurement options to be developed for the enhancement of the power quality control.

On the other hand, the phase information plays a critical role in power systems operation. The phase information was usually extracted through the state estimation (SE) process at the

control room level, where a large amount of measurement is used in this process to obtain coherent picture of the operation of the power system. In many cases the voltage profile in terms of amplitude and phase represents this picture. There are three main limitation for this approach [12]:

- The phase information is the outcome of a numerical process and it is not measured directly.
- Only at the central level, the phase information is available and cannot be used for local processing.
- The state estimation (SE) rate refreshing is slow.

With the growing role of dynamics and the need to operate the power systems closer to their limits, it becomes clear that improving the knowledge of phase quantities is critical to ensure the stability of the whole system.

The principal reason of the development of PMUs are:

- The use of the information for more local process
- The use of a faster and more precise system- level process.

PMUs are measuring devices capable not only of extracting the amplitude of the sinusoidal quantity but also its phase. The estimation of the phase is done by taking Global Positioning System as global time reference that is well known everywhere, the GPS provides an available and reliable time definition. The main obstacle is the choice of the algorithm which is mandatory for extracting the information from a sequence of samples. Many research efforts are carried about this topic and have brought an evolution of the vision of what a PMU really is [11].

1.3.2 Phasor Measurement Unit

The Phasor Measurement Unit is a very efficient measurement technology for power system in monitoring the transmission and distribution conditions of networks [13]. As depicted in Figure 1.3, the phasor is obtained based on sampled analog voltage waveform data, which are synchronized with the GPS receiver clocking signal at both buses (1 & 2). The time reference signal helps to synchronize the waveforms at all buses. The difference in the amplitude between the signals received by the PMUs in both buses is due to the attenuation that occurred to the signal in the transmission line. These synchronized phasor measurements called synchrophasors.

The Global Positioning System GPS receiver is embedded in the PMUs to achieve the synchronization of all the signals in the entire network. These synchrophasors yield to an

instantaneous information about power flow, losses, frequency and other parameters in the power system. Practically, The PMU receives inputs voltage and current waveforms from a standard instrument such as the current transformer (CT) and potential transformer (PT), then the received signals will be isolated, filtered and sampled at an efficient rate of 48 samples per cycle in early devices to as high as 96 or 128 samples in more modern devices.

From the sampled data the PMU's microprocessor uses a Fourier algorithm to compute the physical quantities like the positive sequence, voltage and current phasors and the fundamental frequency. All these quantities are time stamped and will be immediately available via standard communications ports for local or remote applications.

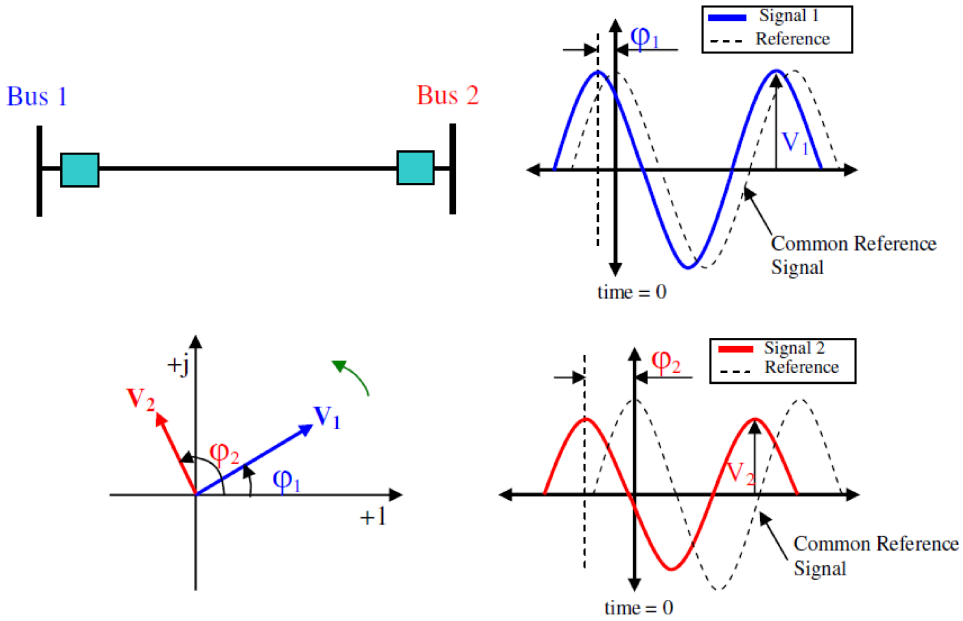

Figure 1.3. *Signal received by PMUs at remote locations [14]*

The purpose of phasor estimation technique based on Fourier algorithm is just used to transform sinusoidal signal to phasor representation. The sampled data used by PMU's based on Fourier algorithm is illustrated in Figure 1.4.

The waveform data samples are collected over data window which normally represents one period of the power system nominal frequency (50/60 Hz). Using the Discrete Fourier Transform (DFT) the phasor can be estimated through the formula shown in the following equation (1.4) [9]:

$$\bar{X} = X_r + jX_i = \frac{\sqrt{2}}{N}\sum_{n=1}^{N}\left(x_n \cos\frac{2n\pi}{N} + jx_n \sin\frac{2n\pi}{N}\right) \quad (1.4)$$

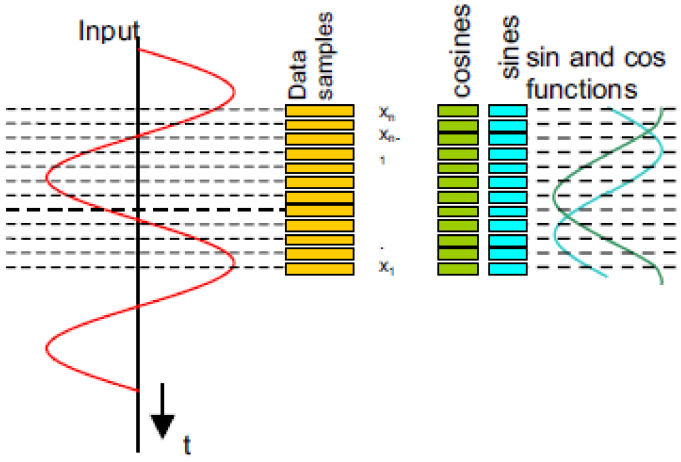

Figure 1.4. *Sampled data for the estimation of phasor [7]*

Where $\bar{X}$ is the synchrophasor, X_r and X_i are the real and imaginary parts of the synchrophasor respectively, N is the number of samples in data window (one period) and x_n is the data of the n^{th} sample. If the input signal frequency differs from the nominal frequency, a correction of magnitude and angle must be applied taking into consideration the deviation in the frequency, the options and secondary corrections are described in [15]. In addition to that the input signal should be filtered according to the Nyquist theorem to avoid aliasing. The majority of PMUs use a multiple cycle window rather than one period data window.

Another efficient method known by recursive Discrete Fourier Transform is used in the estimation of the phasor. In this method, the contribution made by the new sample data is added when the oldest one is subtracted, it is like a moving window as shown in figure 1.5. In the recursive DFT the nominal frequency of constant sinusoid produces a constant phasor.

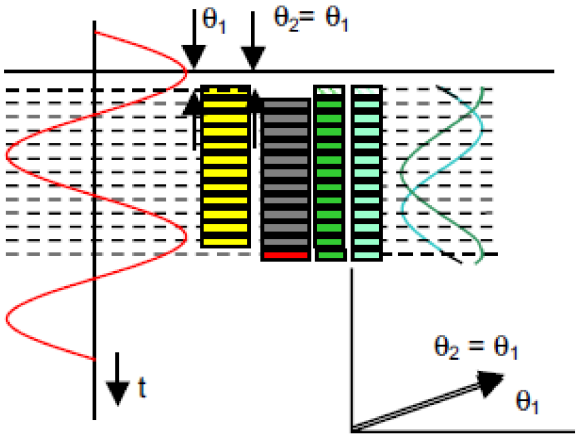

Figure 1.5. *Recursive estimation of phasor [7]*

It is also noteworthy that the early attempt of the PMU to estimate the rate of change of frequency (ROCOF) is based on the frequency obtained by the difference between two consecutive phase angles over time difference. This leads to a noisy estimation of the frequency as well as the ROCOF. A more effective approach is to measure several consecutive phase angles e.g. 3 to 6 periods, then make a suitable polynomial that fits those measured phase angles. The differentiation of polynomial can identify a very good estimation of the frequency and the ROCOF [9].

As the majority of electrical devices the PMU is consisted of software and hardware parts. It is clear that the software parts are represented by the PMU algorithm that will be executed to process the sampled data in order to implement the PMU functions. In the other side, the hardware parts consist of voltage and current transformer for each phase to carry the analog measurement signal to the anti-aliasing filter. The purpose of this filter is to limit the signals with high frequencies, which cannot be supported by the Analog to Digital Converter (ADC) as shown in Figure 1.6. Thus, it is crucial to pass the analog signal through the anti-aliasing filter before data sampling since the sampled data represents the input signal.

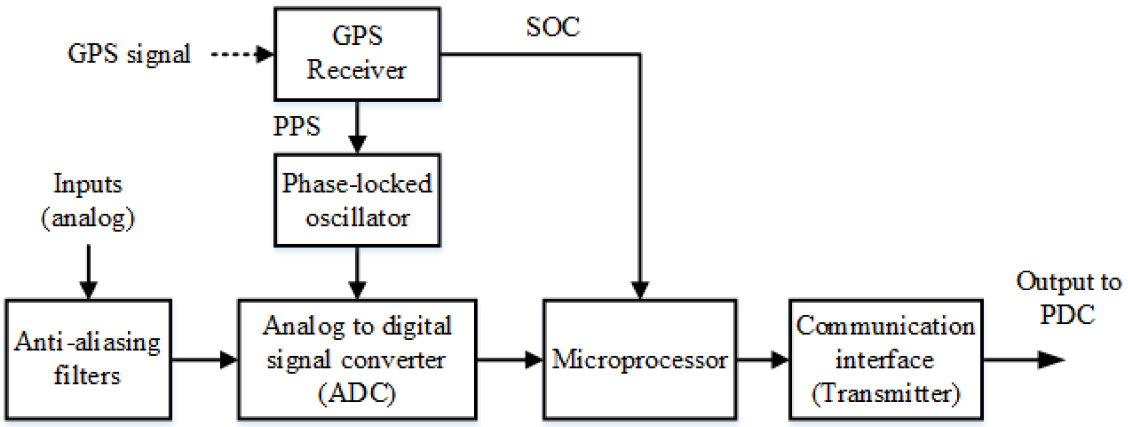

Figure 1.6. *Functional block diagram of the PMU's elements [16]*

The captured phasors are to be time-tagged based on the UTC time reference. The GPS clock signal is received once every second (1 PPS). Within a PMU, a phase-locked oscillator generates the time tags within the second. The time stamp information is an 8-byte message consisting of:

- *4-byte "Second Of Century – SOC":* The SOC time-tag counts the number of seconds that have occurred since inception of PMU (midnight 01-Jan-1970).
- *4-byte "Fraction of Second – FRACSEC":* consist 3-bytes for the Fraction of Second, one second can be divided to 16,777,216 approximately 59.6 ns and 1-byte for time quality

indicator, and it contains information about relative accuracy of the source clock. (4 bits for time error and the other 4 bits for maximum time error).

The data samples and their tag-times are simultaneously sent to the PMU microprocessor to be processed, then an overall message include the phasors and other parameters is sent to the transmitter (communication interface) and then to be served to client application for display, analysis, monitoring and control. If the received phasor information packet from the server/PDC is out of order, the phasor time response can still be correctly assembled since it is stamped with time. Thus, the operators in the central control room can acquire phasor values sequentially and continuously.

The overall message includes a packet of information represented in registers that are sent consecutively. Figure 1.7 illustrates how these registers are ordered to be transmitted consecutively where Table 1.1 illustrates the content of each register.

Table 1.1. *Information packet data [4].*

Field	Size (bytes)	Comments
SYNC	2	Frame synchronization word. Leading byte: AA hex Second byte: Frame type and version, divided as follows: Bit 7: Reserved for future definition, must be 0 for this standard version. Bits 6–4: 000: Data Frame 001: Header Frame 010: Configuration Frame 1 011: Configuration Frame 2 101: Configuration Frame 3 100: Command Frame (received message) Bits 3–0: Version number, in binary (1–15) Version 1 (0001) for messages defined in IEEE Std C37.118-2005 [B6]. Version 2 (0010) for messages added in this revision,IEEEStd C37.118.2-2011.
FRAMESIZE	2	Total number of bytes in the frame, including CHK. 16-bit unsigned number. Range = maximum 65535
IDCODE	2	Data stream ID number, 16-bit integer, assigned by user, 1–65534 (0 and 65535 are reserved). Identifies destination data stream for commands and source data stream for other messages. A stream will be hosted by a device that can be physical or virtual. If a device only hosts one data stream, the IDCODE identifies the device as well as the stream. If the device hosts more than one data stream, there shall be a different IDCODE for each stream.
SOC	4	Time stamp, 32-bit unsigned number, SOC count starting at midnight 01-Jan-1970 (UNIX time base). Range is 136 years, rolls over 2106 AD. Leap seconds are not included in count, so each year has the same number of seconds except leap years, which have an extra day (86 400 s).
FRACSEC	4	Fraction of second and Time Quality, time of measurement for data frames or time of frame transmission for non-data frames. Bits 31–24: Message Time Quality Bits 23–00: FRACSEC, 24-bit integer number. When divided by TIME_BASE yields the actual fractional second. FRACSEC used in all messages to and from a given PMU shall use the same TIME_BASE that is provided in the configuration message from that PMU.
DATA 1...N		Phasors, Frequency, ROCOF…
CHK	2	RC-CCITT, 16-bit unsigned integer.

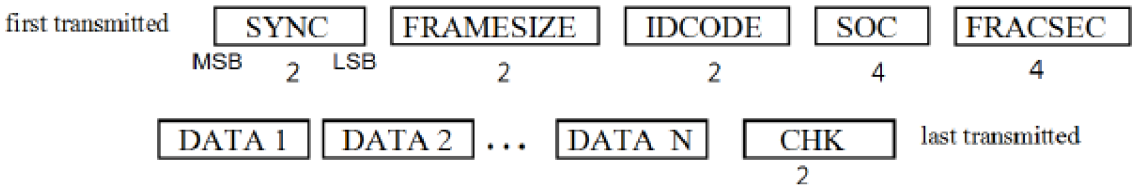

Figure 1.7. *Information packet transmission order [4].*

In Wide Area Measurement System (WAMS), several PMUs are usually located at different connection points (buses) in a large power grid. A Phasor Data Concentrator (PDC) is used to aggregate measurements from these PMUs. In this context, up to 30 PMU signals can be received only by one PDC at the same time and align them according to their time stamp. This can be used in monitoring, protection or control applications for large power systems.

1.3.3 PMU Measurements

PMUs measure synchronously:

- Positive sequence voltages and currents.
- Phases of the positive voltages and currents.
- Local frequency.
- Local rate of change of frequency ROCOF.

1.3.4 Hierarchy of phasor measurement systems

In practice, the phasor data is used at locations far away from the PMUs. In order to realize the great advantages of measurement system based on PMUs there must be an architecture with PMUs, communication means and phasor data concentrations. A generic accepted structure of a WAMS is depicted in Figure 1.8 where the PMUs are in the first level of hierarchy then the secondary are the PDCs and finally the primary PDCs (Super PDCs) and the control centres.

The provided measurements by the PMUs are stored locally in data storage devices, this local storage devices can be accessed by remote locations in order to perform diagnostics or post-mortem. It is obvious that the local storage capacity is limited hence the stored data of an event of interest should be flagged in order to avoid being overwritten. [11]

The devices at the next hierarchical level are PDCs. The role of PDCs is to align the received measurements from PMUs and others PDCs using the time stamp, reject the bad data and feed them as a single stream to other application [18]. The PDCs have also a local storage facilities that store a coherent simultaneously recorded data from a wider part of the system. The sorted measurements can be transmitted to the highest PDC level to share data between control centres. The functions of the highest PDC level are similar to those of other PDCs but it covers

all the entire power system.

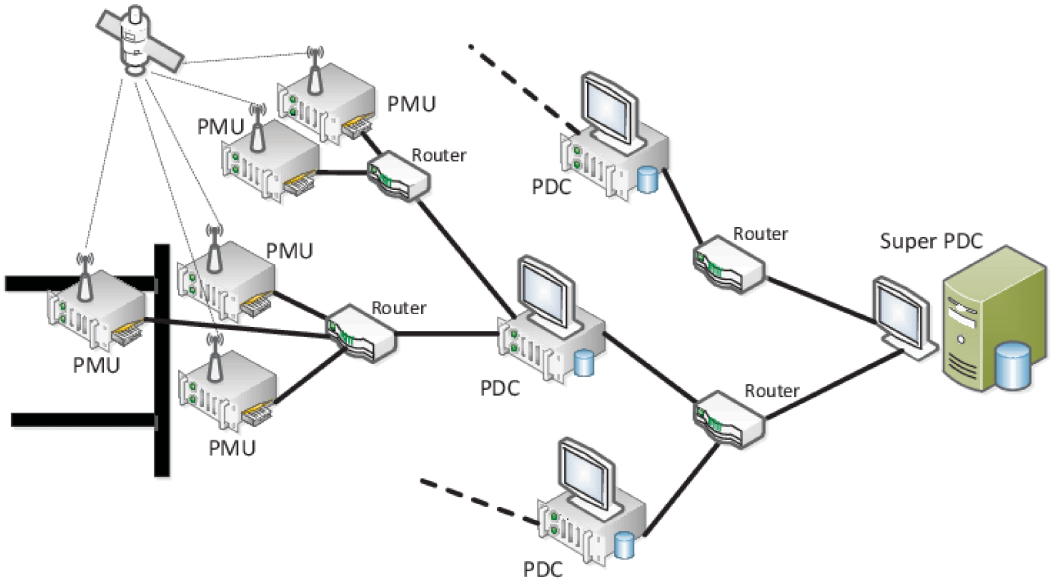

Figure 1.8. *A hierarchical architecture of the wide area measurement system [17]*

1.3.5 PMU connection

A typical PMU connection block diagram is depicted in Figure 1.9, the voltage and current transforms are typically found in substations and generation stations of the power system. This instrument transformers convert the power system voltage and current to a standard secondary level signals to be sent to the PMU through the instrumentation channel which is consisted of control cables and burdens. It is clear that the instrumentation channel will produce an accurate replica of the high voltage or current waveform at the output and scaled by a factor [19].

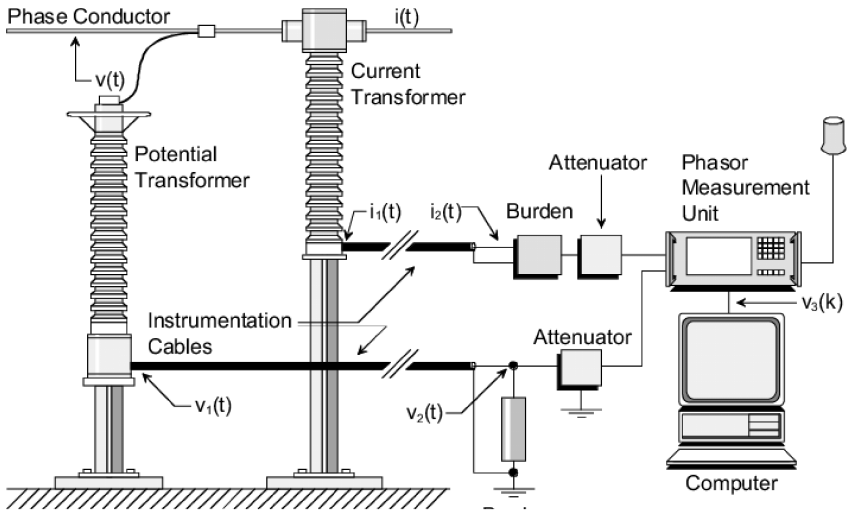

Figure 1.9. *Typical instrumentation channel for PMU data collection [20]*

1.3.6 PMU Performance Criteria

The accuracy of synchrophasor measurement has been described by the Total Vector Error (TVE) that was introduced in IEEE C37.118-2005 [21].The errors in the synchrophasor measurement may result from errors in magnitude or phase, or both. The TVE combines the two types of errors in one measure and which is defined as follows:

$$TVE = \sqrt{\frac{(X_r(n) - X_r)^2 + (X_i(n) - X_i)^2}{X_r^2 + X_i^2}} \tag{1.5}$$

Where $X_r(n)$ and $X_i(n)$ are the real and imaginary parts of the syncrophasor measured value given by the PMU, X_r and X_i are the real and imaginary parts of the theoretical input signal at the instant of measurement time.

According to IEEE C37.118.1-2011 standard, TVE requirements are expanded by adding new dynamic performance tests. As an example, in a steady state conditions at nominal amplitude and frequency a TVE less than 0.01 % should be achieved [4,22]. In addition to that, the measurements of frequency and ROCOF are evaluated as the difference between the measured values of the PMU and the reference values of the same time, these are defined as follows [9]:

- Frequency Error: $$FE(n) = f_{measured}(n) - f_{ref}(n) \tag{1.6}$$

- ROCOF Error: $$RFE(n) = \frac{df}{dt}_{measured}(n) - \frac{df}{dt}_{ref}(n) \tag{1.7}$$

1.4 Wide Area Measurement System (WAMS)

An accurate and comprehensive definition of WAMS was introduced by Hauer from BPA/Pacific NW National Labs, this definition states that the WAMS is a strategic effort to meet critical information of the power system changing. It is also mentioned that an infrastructure is needed for the WAMS, according to Hauer this infrastructure is made up of people, operating practices, negotiated sharing arrangements and everything else necessary to provide useful information for WAMS facilities.

Nowadays, PMUs are commercially available and extensively used in power grids because of the great benefits of the PMUs over the classical measurement systems. Therefore, the WAMS definition differs little bit from that of the past. Thus as a new definition, the WAMS combines the provided data from synchrophasor and conventional measurements for monitoring, controlling, operating and protecting wide geographical power systems with the capability of new communication systems [23].

As it is mentioned previously in section 1.3.4, the PMU measurements are sent to a PDC at a rate up to 60 frame per second with modern technology PMUs. The PDC gathers all the PMUs data to a single frame to be transmitted to any WAMS-based application. A general and practical WAMS architecture diagram includes some applications is depicted in Figure 1.10.

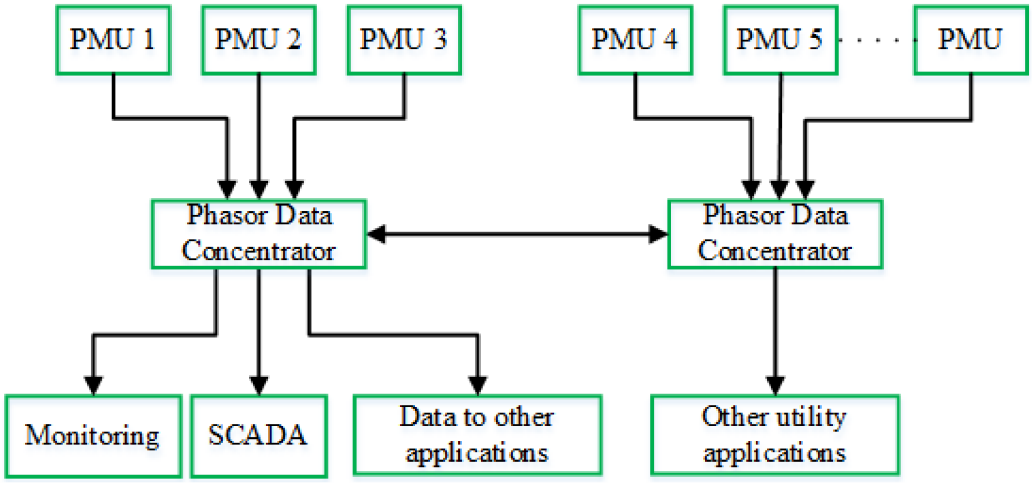

Figure 1.10. *WAMS architecture include some applications [24]*

1.5 Overview about Power System State Estimation

In 1970, Fred Schweppe introduced the use of State Estimation in power systems to obtain a clear picture of the transmission network operating conditions [25]. According to Fred the SE procedure is the result of the combination of statistical estimation theory and load flow analysis. Classically, the voltage angles and magnitudes at all the buses of the entire network define the state of the power system. Thus, State Estimation is defined as a mathematical approach which permits estimating the most likely operating status of the network based on the processing of resource data (network and measurement data).

Nowadays, SE is becoming increasingly based on PMU measurements rather than the conventional measurement systems. Once the network state is known, all the required electrical quantities can be calculated and any management or control functions can be carried out. In reality, many events always occur, which effect the performance of the State Estimation process like the uncertainty and the unavailability of measurement, the bad data, the malfunction of devices, the communication errors … etc. In order to overcome these problems, an appropriate processing stages are needed to remove all the bad and erroneous data. State Estimators typically includes the applications represented in the flowchart of Figure 1.11 and clarified beneath [12, 26]:

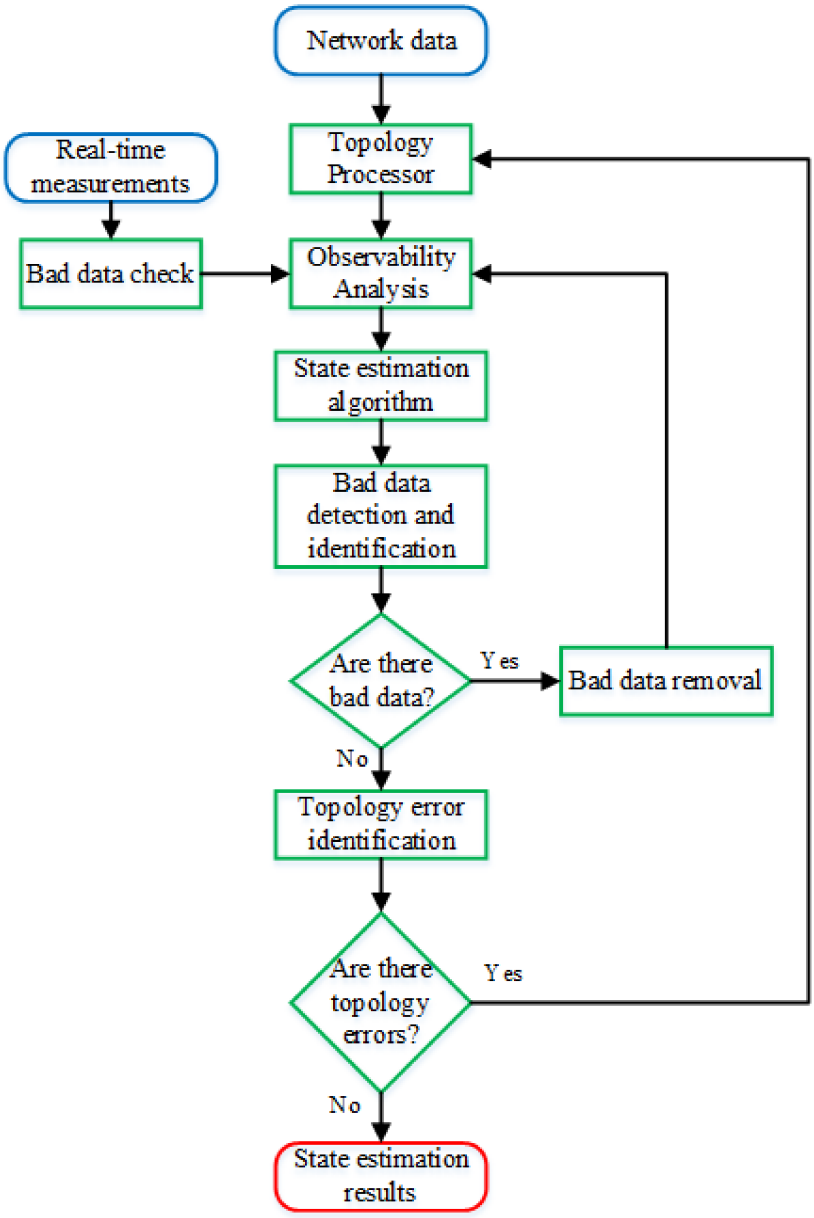

Figure 1.11. *Typical flowchart of state estimation [12]*

- Topology processor: builds the topology of the network from the states of circuit breakers and switches.

- Observability analysis: Determines whether the available measurement set can be used to obtain a state estimation solution for the whole system or not. If it is not possible, It is necessary to detect observable islands in order to allow the SE to run at least on them.

- State Estimation algorithm: it is the heart of the state estimator. Based on the network model and the collected real-time measurements the SE algorithm determines the system state estimation which is composed of complex bus voltages in addition to the estimations for line current flows, transformer taps, loads, and generator outputs.

- Bad data processing: Detects, identifies and then discards the bad and erroneous data given that the measurement configuration is sufficiently redundant. The bad data processing can be included in the SE algorithm. It is also possible to perform a bad data check before the execution of the SE algorithm to reject senseless measurements immediately e.g. negative voltage or current magnitudes.

- Parameter and structural error processing: it analyses the estimation results to determine the parameters of the network topology, then it identifies the possible errors in the assumed topology which is obtained from the topology processor. These errors can be due to bad or missed communication of switch state.

Power systems SE determines the state of the power grid from its mathematical model and the collected real-time measurements. The estimation can be performed using various SE algorithms such that: static state estimation, weighted least squares methods (WLS), linear state estimation …etc. In addition to fuzzy logic based SE, artificial neural network based SE…etc. [12].

It's also worthy of note that PMUs enhance significantly the quality of SE results as well as the Energy Management System (EMS) due to the provided accurate synchronized measurements.

1.6 The comparisons between SCADA system and PMUs system

The main differences between SCADA and PMUs systems are given in the following Table:

Table 1.2. *SCADA & PMU main differences [24]*

	SCADA	PMU
Measured quantities	Magnitude only	Magnitude and phase angle
Time synchronization	No	Yes
Resolution	1 sample every 2-4 seconds	Up to 60 samples per second
Observability	Steady state observability	Dynamic observability
Focus	Local monitoring and control	Wide area monitoring and control

As an example for the difference in measurement resolution between the SCADA and PMU systems Figure 1.12 shows the measurement of both systems during a fault-induced delayed voltage recovery (FIDVR) event that refers to unexpected delay in the recovery of voltage to

its nominal value after the normal clearing of a fault. In this case the PMUs system shows almost every detail with high resolution whereas the SCADA system couldn't detect the voltage drop before the voltage swell. Also as it is shown in Figure 1.13, the SCADA system has difficulties with voltage oscillations detection.

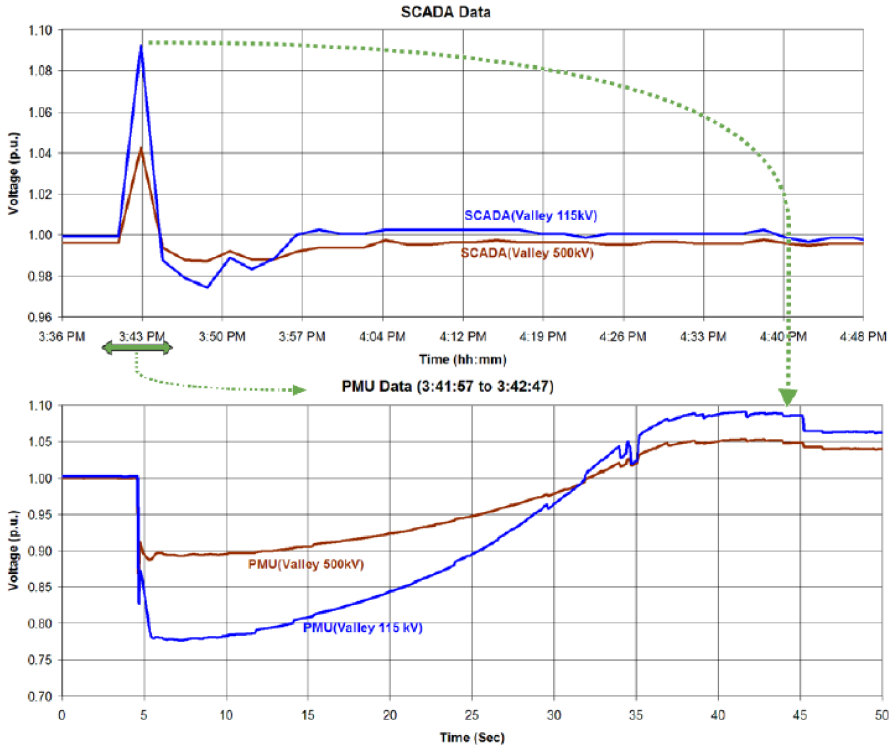

Figure 1.12. *SCADA and PMU measurements during a fault-induced delayed voltage recovery (FIDVR) event [27]*

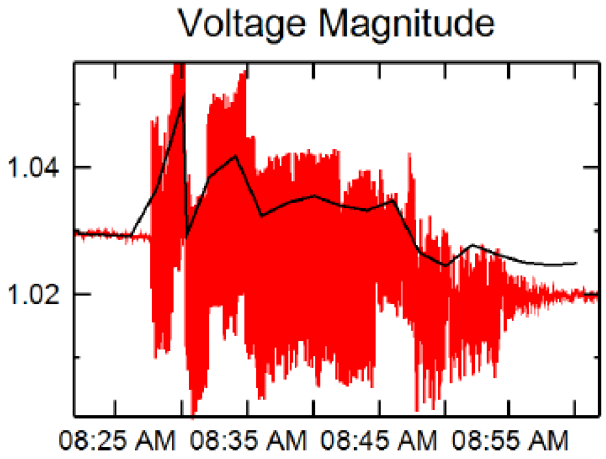

Figure 1.13. *SCADA and PMU measurements during voltage oscillations [28]*

1.7 PMU challenges

As any new technology, Phasor Measurement Units encounter many challenges such as:

- Visualization of PMU data: Difficult to visualize and manage the voluminous data.
- Communication of PMU data: High-cost communication network.
- Initial high investment requirement acts as an obstacle.
- **Optimal Placing of PMUs.**

1.8 Conclusion

PMUs are being commercially manufactured by several companies and it is obvious that the most major power systems will adopt this technology due to the increased development and interest on using the WAMS around the world. PMUs offer attractive options for enhancing protection and control actions of modern power systems in addition of ensuring more precise and accurate of their state estimation.

In order to monitor the dynamics of the power system, PMU provides coherent high - speed data that are not available with traditional SCADA measurements. Furthermore, the angle measurements are made directly by the PMU while SCADA system uses the measurements of voltage, active power, reactive power and a reference angle. Besides that the most important point is that the PMU measurements are time synchronized.

CHAPTER 2

Optimal PMU Placement Formulation

- *Introduction*
- *Power system observability*
- *PMU based network observability rules*
- *Optimal PMU Placement (OPP) problem formulation*
- *System Observability Redundancy Index (SORI)*
- *Example of constraint vector function formulation*
- *Conclusion*

Optimal PMU Placement Formulation

2.1 Introduction

A. G. Phadke has proposed in his research work that the reliability of the power network could be substantially improved by installing PMUs at all substations [29]. Thus, an adequate criteria that reflects the trade-off between the technical advantages and financial costs should be found. The financial cost does not include only the PMU devices cost but also the installation costs and the communication infrastructure costs. To reduce the unit costs and its maintenance fees, the number of installed PMUs should be reduced under the constraint of ensuring an entire degree of observability of the whole concerned power system. The investigation to find the required minimum number of PMUs while keeping the full observability of the power system referred to as the optimal PMUs placement (OPP) problem.

Several researchers have developed methods based on the observability analysis of the power system to determine the optimal placement of PMUs. These methods carry out an optimization process that takes all system buses into account.

The analysis of power system observability can be categorized into numerical and topological analysis. The numerical analysis is based on whether the matrix (H) presented in equation (2.2) that relates measurements to bus voltage magnitudes and angles is of full rank or not. Whereas, the topological analysis is based on the graph theory i.e. the network is observable if and only if there exists a spanning tree of full rank [30, 31].

The buses to be equipped with PMUs are of important consideration in the development of PMU placement techniques according to the restrictions and provided data by the measuring devices.

Topological observability is adopted in this **project** where the required information is the network connectivity, zero injection buses and their locations.

2.2 Power system observability

A given power network can be fully observed if all buses can be observed by direct or indirect measurement based on KCL and KVL. There are two different approaches, which are used for system observability, the numerical observability and the topological observability.

2.2.1 Numerical observability

A power system with M measurements and N nodes can be described by the classical formulation of the state estimation as follows [30]:

$$Z = h(x) + e \quad (2.1)$$

Where Z is the measurement vector of M dimensions, x is the state vector that includes the voltage angles and magnitudes of all buses except the reference angle, hence its dimension is 2N-1, e is the measurement error vector which has the same dimension as Z , $h(x)$ is a vector function that relates the state vector x to the measurement vector Z, it is called also the gain matrix.

Equation (2.1) can be rewritten as follows:

$$Z = H.x + e \quad (2.2)$$

Where H is the Jacobian matrix of $h(x)$.

A system is algebraically observable if its model can be solved for the state estimation. According to equation (2.2), the system is algebraically observable if the matrix H is of full rank and it is well-conditioned [32].

It is worthy to note that in case of large power systems the Jacobian matrix can become mal-conditioned and lead to low computational speed.

2.2.2 Topological observability

The network observability can be determined through topological algorithms. These algorithms use the graph theory and besides that they are based only on the measurement types and their locations in the whole system. An N-bus system can be observed topologically if its measurements are placed in such a way that there is at least one spanning tree of full rank [30, 33].The Methods based on topological observability ensure complete topological observability but do not ensure that the Jacobian Matrix (H) is of full rank [34].According to the measurement type the topological observability algorithms can be classified into conventional and PMU based observability algorithms.

The concept of topological observability through conventional measurements was introduced firstly in [33].Conventional observability algorithms use real / reactive power flows, power injections, bus voltage magnitudes and branch currents. In the other hand, the PMU based observability algorithms use the measurement provided by the PMUs, which are different compared to the conventional metering devices, PMUs can obtain the voltage and current phasors of the entire system at once, because PMUs can offer synchronized phasor measurements in real time through global positioning system (GPS).

This project deals with the **PMU based topological observability** where the problem formulation is derived based on the topological observability rules.

2.3 PMU based network observability rules

A power system is observable if all the voltages of its buses are known, assuming that the PMU can measure all the line currents connected to the PMU bus. The voltage and branch currents of a bus where the PMU is installed are measured directly. Whereas, in bus without PMU installed it can be measured indirectly using KCL and KVL based on other known parameters such as other bus voltages and branch currents.

In order to ensure that the network is fully observable, several rules are applied for the analysis of the network. The following details the observability rules used to determine the power system observability based on the fundamental laws in circuit theory of node voltage and branch current:

Rule 1:

A PMU installed bus will have its voltage phasor and current phasors of all its incident branches directly measured by the PMU. These are referred to as "direct measurement". Consider Figure 2.1, where the PMU is installed at bus 1, accordingly, the bus voltage V_1 and the branch currents I_{12},I_{13} , I_{14} can be directly measured by the PMU.$R_{12} + jX_{12}$, $R_{13} + jX_{13}$ and $R_{14} + jX_{14}$ are the provided characteristics of transmission lines 1-2, 1-3 and 1-4 respectively.

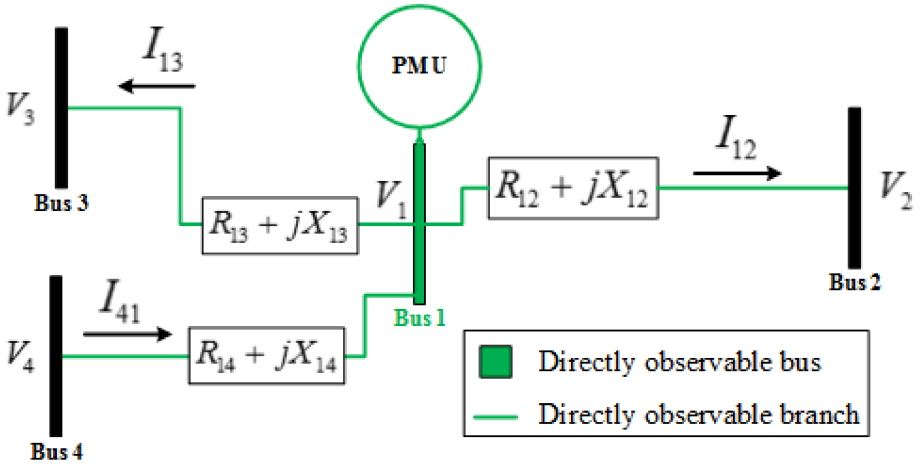

Figure 2.1. *Observability rule 1*

Rule 2:

If the voltage and current phasors are known at one end of a branch, the voltage phasor can be obtained at the other end of the branch just by calculation. These are referred to as "pseudo measurement". Consider Figure 2.2, as it is mentioned previously in rule one the values V_1 ,I_{12} ,I_{13} andI_{14} are known in addition to the transmission line parameters. Using Ohm's law

the buses' voltages V_2, V_3 and V_4 can be calculated through the equations (2.3), (2.4) and (2.5).

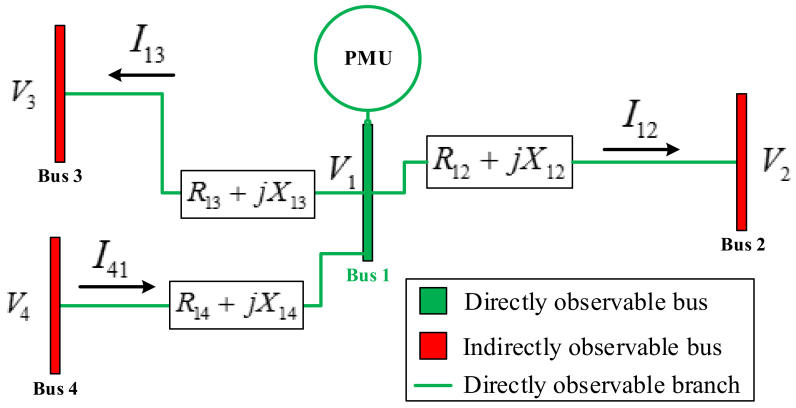

Figure 2.2. *Observability rule 2*

$$V_2 = V_1 - I_{12}(R_{12} + jX_{12}) \quad (2.3)$$
$$V_3 = V_1 - I_{13}(R_{13} + jX_{13}) \quad (2.4)$$
$$V_4 = V_1 + I_{14}(R_{14} + jX_{14}) \quad (2.5)$$

Rule 3:

In case where the voltage phasors are known at both ends of a branch, this branch current can be calculated using Ohm's law. Consider Figure 2.3, the buses 1 and 2 are observed by PMUs installed in other neighbouring buses. Thus, V_1 and V_2 are known, hence the current flowing between these buses is unknown. This current can be calculated following equation (2.6).

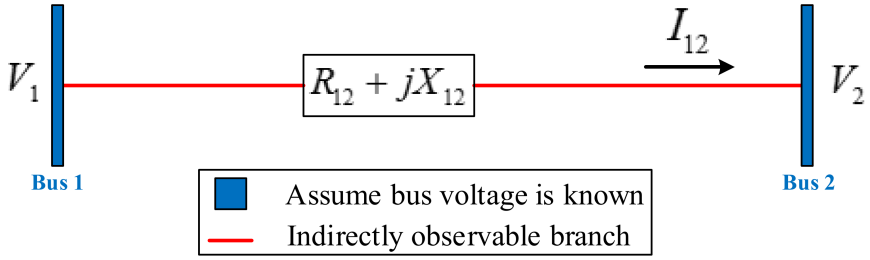

Figure 2.3. *Observability rule 3*

$$I_{12} = \frac{V_1 - V_2}{R_{12} + jX_{12}} \quad (2.6)$$

2.3.1 Observability rules considering ZIB

A bus where neither load nor generator is connected, is referred to as Zero Injection Bus (ZIB). By other words, the injected power to this bus is equal to zero. Therefore, the sum of branch currents is zero according to KCL. A ZIB and its neighbour buses are of N numbers, thus it is sufficient to observe $N - 1$ buses to make the non-observable bus observable. Hence,

by taking into consideration the ZIBs, the number of buses to be observed will be reduced by one for each ZIB. Thereby reducing the number of PMUs required for full observability.

The following observability rules are applied to assess topological observability when considering Zero Injection Bus (ZIB):

Rule 4:

If there is an indirectly observable zero injection bus and the voltage phasors of the adjacent buses are all known except one, the voltage phasor of the unknown bus can be calculated using KCL. Consider Figure 2.4, bus 2 is the observable zero injection bus, also bus 1 and 2 are observable. Hence, V_1 , V_2 and V_3 are all known. Using rule 3 the branch currents I_{12} and I_{23} can be calculated. The current I_{24} is found by applying KCL at the ZIB and consequently V_4 according to the following equations:

$$I_{24} = I_{12} - I_{23} \tag{2.7}$$

$$V_4 = V_2 - I_{24}(R_{24} + jX_{24}) \tag{2.8}$$

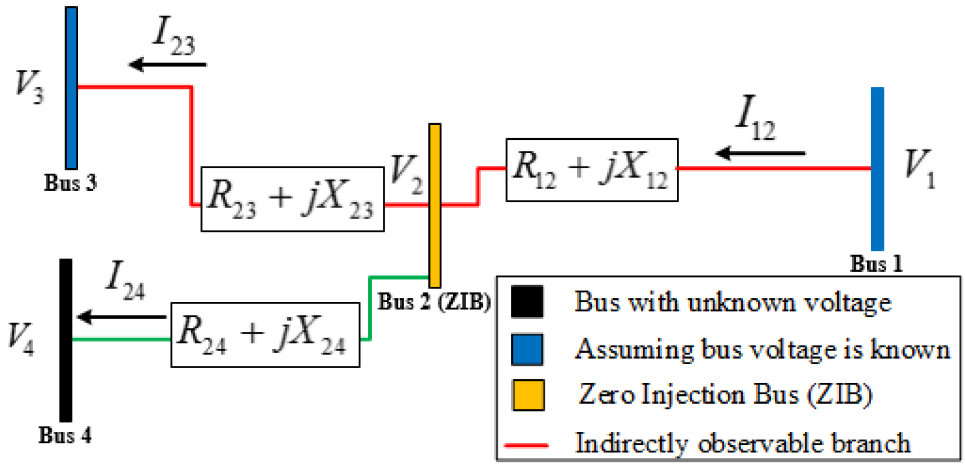

Figure 2.4. *Observability rule 4 when considering ZIB*

Rule 5:

If a ZIB voltage phasor is not known and the voltage phasors of all its neighbouring buses are known, the ZIB voltage phasor can be obtained via the node voltage equations. Consider Figure 2.5, bus 2 is the unobservable ZIB where all the adjacent buses are observable. The unobservable ZIB voltage phasor can be computed by solving the following system of equations:

$$\begin{cases} V_2 = V_1 - I_{12}(R_{12} + jX_{12}) \\ V_2 = V_3 + I_{23}(R_{23} + jX_{23}) \\ V_2 = V_4 + I_{24}(R_{24} + jX_{24}) \\ I_{12} = I_{23} + I_{24} \end{cases} \tag{2.9}$$

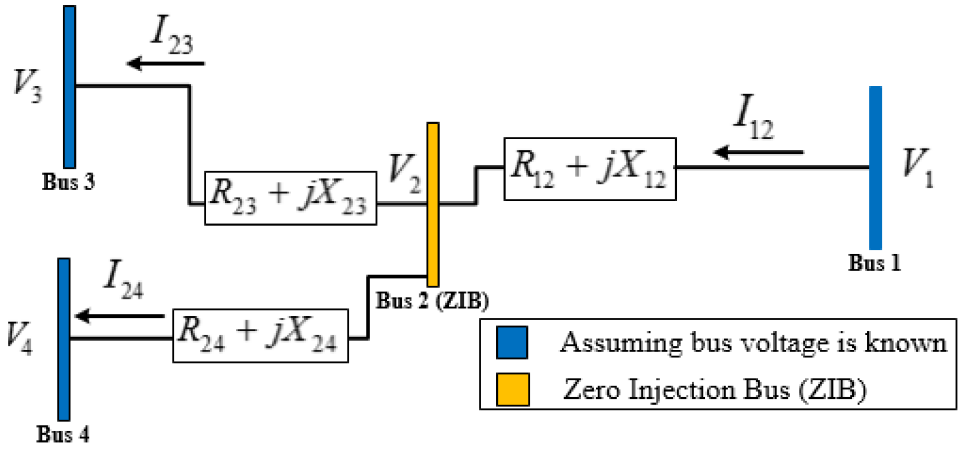

Figure 2.5. *Observability rule 5 when considering ZIB*

Rule 6:

Is just a developed version of the previous rule (Rule 5). If there are unobservable connected ZIBs and all their adjacent buses are observed, the ZIBs' voltages can be computed using node equations. Consider Figure 2.6, where buses 5 and 4 are ZIBs and the other buses are indirectly observable, hence $V_4$and V_5 can be obtained by solving the following system of equations:

$$\begin{cases} \dfrac{V_5 - V_4}{R_{54} + jX_{54}} + \dfrac{V_5 - V_1}{R_{51} + jX_{51}} + \dfrac{V_5 - V_6}{R_{56} + jX_{56}} = 0 \\ \dfrac{V_4 - V_5}{R_{54} + jX_{54}} + \dfrac{V_4 - V_3}{R_{43} + jX_{43}} + \dfrac{V_4 - V_2}{R_{42} + jX_{42}} = 0 \end{cases} \tag{2.10}$$

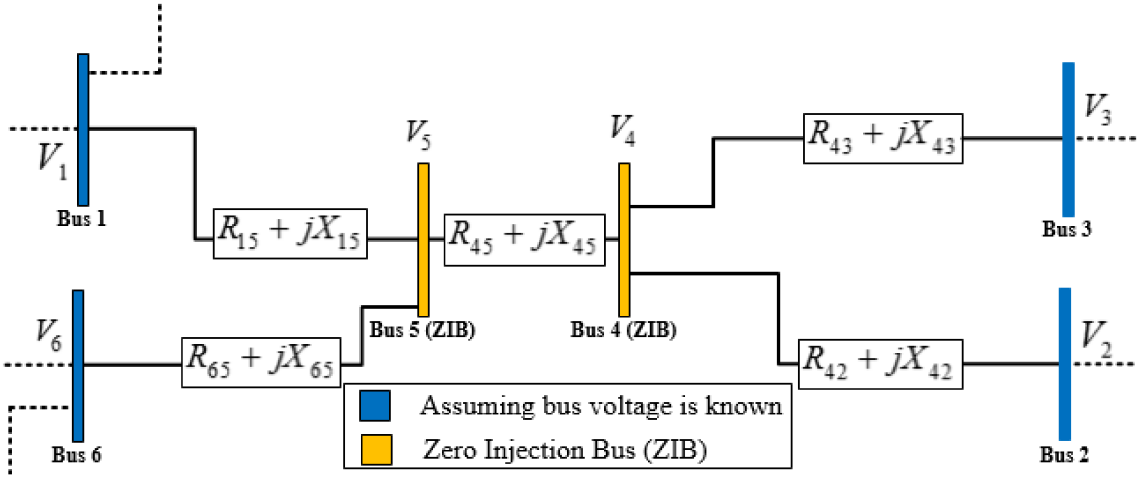

Figure 2.6. *Observability rule 6 when considering ZIB*

2.4 Optimal PMU Placement (OPP) problem formulation

The system topology and type of system buses are sufficient to find the optimal locations of PMUs. A connectivity matrix describes the system bus connections, this matrix shows how buses are interconnected by transmission lines. If the number of buses is N, then the connectivity matrix will be of dimension $N \times N$ with the following entries:

$$[A]_{ij} = a_{ij} = \begin{cases} 1, & if\ i = j \\ 1, & if\ busses\ i\ and\ j\ are\ connected \\ 0, & otherwise \end{cases} \quad (2.11)$$

The nature of the optimal PMU problem requires the following definition of the binary variable vector X:

$$x_i = \begin{cases} 1, & if\ a\ PMU\ is\ installed\ at\ bus\ i \\ 0, & otherwise \end{cases} \quad (2.12)$$

The determination of the placement of the required PMUs to achieve the full observability with minimum cost can be modelled by a constrained optimization problem. The objective function is to minimize the total cost of PMUs to be placed, whereas the involved constrain is that each node in the network should be at least observed by one PMU. The optimization problem can be formulated as follows [35]:

$$\min\left(\sum_{i=1}^{N} w_i x_i\right)\ s.t:\ f_i \geq 1\ ;\ i = 1 \dots n \quad (2.13)$$

Where:

- w_i is the total installation cost of the PMU at bus i,
- f is a vector function representing the constraints, it expresses the observability of each node, and its entries are as follows:

$$f_i \begin{cases} \neq 0, if\ node\ i\ is\ observable \\ = 0, if\ node\ i\ is\ unobservable \end{cases} \quad (2.14)$$

The PMU cost depends on a many factors, including the number of measurement channels, connections of CT and PT, ground connection, power connection and the GPS receiver [34]. Assume that the cost of all PMUs is equal. Therefore, the objective function will be as follows:

$$\min\left(\sum_{i=1}^{N} x_i\right)\ s.t: f_i \geq 1 \quad i = 1 \dots n \quad (2.15)$$

The observability of each bus can be expressed by the vector function $f(X)$ through a set of linear equations derived from the multiplication between the connectivity matrix A and the binary variable vector X .

$$f(X) = A.X \tag{2.16}$$

Where: $$X = [x_1, x_2, x_3, \dots, x_N]^T \tag{2.17}$$

The example shown below in Figure 2.7 can be used to clarify the classical optimization problem formulation.

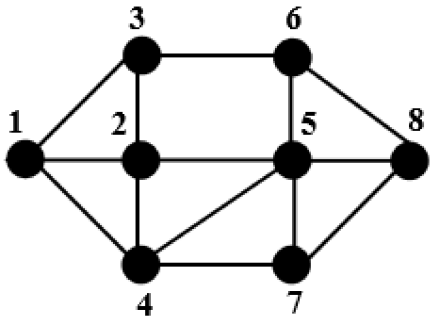

Figure 2.7. *Network topology for 8-bus system*

The corresponding network connectivity matrix A is as follows:

$$A = \begin{bmatrix} 1 & 1 & 1 & 1 & 0 & 0 & 0 & 0 \\ 1 & 1 & 1 & 1 & 1 & 0 & 0 & 0 \\ 1 & 1 & 1 & 0 & 0 & 1 & 0 & 0 \\ 1 & 1 & 0 & 1 & 1 & 0 & 1 & 0 \\ 0 & 1 & 0 & 1 & 1 & 1 & 1 & 1 \\ 0 & 0 & 1 & 0 & 1 & 1 & 0 & 1 \\ 0 & 0 & 0 & 1 & 1 & 0 & 1 & 1 \\ 0 & 0 & 0 & 0 & 1 & 1 & 1 & 1 \end{bmatrix} \tag{2.18}$$

From equations (2.16), (2.17) and (2.18), the constraint vector function to be verified for the placement solution is:

$$f(X) = \begin{cases} f_1 = x_1 + x_2 + x_3 + x_4 \geq 1 \\ f_2 = x_1 + x_2 + x_3 + x_4 + x_5 \geq 1 \\ f_3 = x_1 + x_2 + x_3 + x_6 \geq 1 \\ f_4 = x_1 + x_2 + x_4 + x_5 + x_7 \geq 1 \\ f_5 = x_2 + x_4 + x_5 + x_6 + x_7 + x_8 \geq 1 \\ f_6 = x_3 + x_5 + x_6 + x_8 \geq 1 \\ f_7 = x_4 + x_5 + x_7 + x_8 \geq 1 \\ f_8 = x_5 + x_6 + x_7 + x_8 \geq 1 \end{cases} \tag{2.19}$$

In equation (2.19), The operator " + " indicates a logical "OR" and the value of 1 on the right side of the constraints shows that at least one of the binary variables included in each constraint equation must be nonzero e.g. the observability of bus 4 can only be achieved by placing a PMU at least in one of the following nodes 1, 2, 4, 5 and 7.

2.5 System Observability Redundancy Index (SORI)

The redundancy is usually important factor in selecting the optimal PMU placement among the multiple solutions with a given minimum number of PMUs because it enhances the

observability. Hence, the reliability of the power system will be increased. Bus Observability Index (BOI_i) represents the actual number of PMUs which are able to observe bus i.

$$BOI = [BOI_1, BOI_2, BOI_3, \dots\dots, BOI_N] \tag{2.20}$$

The maximum value of BOI_i is limited to maximum number of branch currents connected to bus i (τ_i) plus one.

$$BOI_i \leq \tau_i + 1 \tag{2.21}$$

The System Observability Redundancy Index (SORI) was proposed as shown in equation (2.22) to distinguish between multiple solutions with the same cost [35], it indicates the level of system observability.

$$SORI = \sum_{i=1}^{N} BOI_i \tag{2.22}$$

To choose the best solution among multiple optimal solutions, the one with the highest value of SORI should be selected. Consequently, another objective function is introduced when the redundancy (SORI) is taken into consideration. The goal of this objective function is to maximize the SORI.

$$\max(SORI) = max\left(\sum_{i=1}^{N} BOI_i\right) \tag{2.23}$$

As an example, it is given that the full observability of the network shown in Figure 2.8 can be obtained using a minimum number of 2 PMUs.

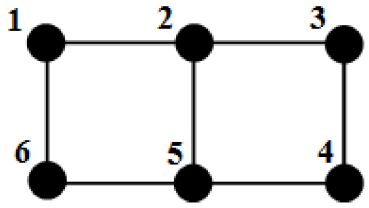

Figure 2.8. *Network topology for 6-bus system*

The placement of PMUs at nodes 1 and 4 is one of the possible solutions. In this case:

$$X = [1,0,0,1,0,0]$$
$$BOI = [1,1,1,1,1,1] \tag{2.24}$$
$$SORI = 1 + 1 + 1 + 1 + 1 + 1 = 6$$

As an alternative solution for the previous case is the placement of the two PMUs at nodes 2 and 5. In this case:

$$X = [0,1,0,0,1,0]$$
$$BOI = [1,2,1,1,2,1] \tag{2.25}$$
$$SORI = 1 + 2 + 1 + 1 + 2 + 1 = 8$$

From this example, it can be noted that a higher level of redundancy is obtained in the second case using the same number of PMUs. Therefore, the second solution is preferred to the 6-bus network as shown in Figure 2.8.

2.6 Example of constraint vector function formulation

In this example, the constraint vector function $f(X)$ will be formulated in both cases of ignoring and considering the zero injection bus for the same network which is shown in Figure 2.9.

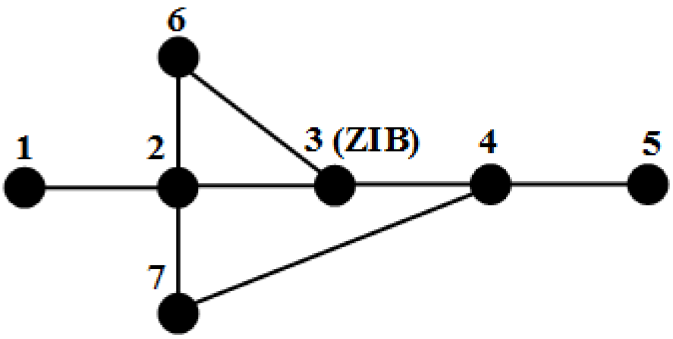

Figure 2.9. *Network topology for 7-bus system*

2.6.1 Constraint vector function formulation when ZIB is ignored

The connectivity matrix A for the 7-bus system shown in Figure 2.9 is as follows:

$$A = \begin{bmatrix} 1 & 1 & 0 & 0 & 0 & 0 & 0 \\ 1 & 1 & 1 & 0 & 0 & 1 & 1 \\ 0 & 1 & 1 & 1 & 0 & 1 & 0 \\ 0 & 0 & 1 & 1 & 1 & 0 & 1 \\ 0 & 0 & 0 & 1 & 1 & 0 & 0 \\ 0 & 1 & 1 & 0 & 0 & 1 & 0 \\ 0 & 1 & 0 & 1 & 0 & 0 & 1 \end{bmatrix} \tag{2.26}$$

By ignoring the ZIB (bus 3) this means that all the buses are considered to be simple buses. Therefore, the constraint vector function according to equation (2.16) can be formed as follows:

$$f(X) = A.X = \begin{cases} f_1 = x_1 + x_2 \geq 1 \\ f_2 = x_1 + x_2 + x_3 + x_6 + x_7 \geq 1 \\ f_3 = x_2 + x_3 + x_4 + x_6 \geq 1 \\ f_4 = x_3 + x_4 + x_5 + x_7 \geq 1 \\ f_5 = x_4 + x_5 \geq 1 \\ f_6 = x_2 + x_3 + x_6 \geq 1 \\ f_7 = x_2 + x_4 + x_7 \geq 1 \end{cases} \tag{2.27}$$

2.6.2 Constraint vector function formulation when ZIB is considered

In this case, bus 3 is considered to be ZIB. According to rules 4 and 5 of observability, it is enough to know the phasor voltages at any three out of the four buses 6, 4, 3 and 2, then the fourth one will be indirectly observable. Therefore, the constraints associated with the previous mentioned buses must be modified a little bit as illustrated below where the operator "." indicates a logical "AND":

$$f_2 = x_1 + x_2 + x_3 + x_6 + x_7 + f_3.f_4.f_6 \tag{2.28}$$

$$f_4 = x_3 + x_4 + x_5 + x_7 + f_2.f_3.f_6 \tag{2.29}$$

$$f_6 = x_2 + x_3 + x_6 + f_2.f_3.f_4 \tag{2.30}$$

The expressions f_2 ,f_4 and f_6 can be simplified using the Boolean algebra properties. Let's take $f_2$as an example, substituting f_3 of equation (2.27) into equation (2.28):

$$\begin{gathered} f_2 = x_1 + x_2 + x_3 + x_6 + x_7 + (x_2 + x_3 + x_4 + x_6).f_4.f_6 \\ f_2 = x_1 + x_2 + x_3 + x_6 + x_7 + x_4.f_4.f_6 \end{gathered} \tag{2.31}$$

Substituting f_4 of equation (2.27) into equation (2.31):

$$\begin{gathered} f_2 = x_1 + x_2 + x_3 + x_6 + x_7 + x_4.(x_3 + x_4 + x_5 + x_7).f_6 \\ f_2 = x_1 + x_2 + x_3 + x_6 + x_7 + x_4.f_6 \end{gathered} \tag{2.32}$$

Substituting f_6 of equation (2.27) into equation (2.32):

$$\begin{gathered} f_2 = x_1 + x_2 + x_3 + x_6 + x_7 + x_4.(x_2 + x_3 + x_6) \\ f_2 = x_1 + x_2 + x_3 + x_6 + x_7 \end{gathered} \tag{2.33}$$

Applying the same logic simplification to all other expressions will yield to the following equation:

$$\begin{gathered} f_2 = x_1 + x_2 + x_3 + x_6 + x_7 \\ f_4 = x_2 + x_3 + x_4 + x_5 + x_6 + x_7 \\ f_6 = x_2 + x_3 + x_6 + x_1.x_4 + x_4.x_7 \end{gathered} \tag{2.34}$$

All the other constraints associated to other buses will remain the same, except the constraint of the ZIB (bus 3) will be eliminated because its effect is already included indirectly in the constraints associated with neighbouring buses (f_2,f_4 and f_6).Hence, the constraint vector function will be as follows:

$$f_{ZIB}(X) = \begin{cases} f_1 = x_1 + x_2 \geq 1 \\ f_2 = x_1 + x_2 + x_3 + x_6 + x_7 \geq 1 \\ f_4 = x_2 + x_3 + x_4 + x_5 + x_6 + x_7 \geq 1 \\ f_5 = x_4 + x_5 \geq 1 \\ f_6 = x_2 + x_3 + x_6 + x_1.x_4 + x_4.x_7 \\ f_7 = x_2 + x_4 + x_7 \geq 1 \end{cases} \tag{2.35}$$

2.7 Conclusion

The background of the OPP problem and how the PMU enhances the monitoring of the power system are presented in this chapter. The observability rules are explained in addition to the rules corresponding to the case of considering the zero-injection buses. OPP problem is formulated as an objective function that allows obtaining the minimum number of PMUs, and a constraint vector function that ensures full observability of the power system.

The OPP problem is an optimization problem, hence an optimization algorithm should be used to solve this problem. In the present work the meta-heuristic and heuristic algorithms, are proposed to be applied for solving the aforementioned optimization problem. These algorithms are presented in the next chapter.

CHAPTER 3

Meta-heuristic Algorithms

- *Introduction*
- *Proposed Meta-heuristic Algorithms*
- *General optimization problem statement*
- *Particle Swarm Optimization (PSO)*
- *Grey Wolf Optimizer (GWO)*
- *Moth Flam Optimization (MFO)*
- *Cuckoo Search (CS) via Lévy flights*
- *Wind Driven Optimization (WDO)*
- *Conclusion*

Meta-heuristic Algorithms

3.1 Introduction

In the optimization of engineering problems, the objective functions are usually very complex, nonlinear and multi-dimensional (multi-variable). The simple calculus concepts using the Differentiation Integration based on analytic evaluation cannot be applied to solve this kind of problems for finding points of global maximum or global minimum. This leads to introduce the use of nonlinear programming based on mathematical programming technique which helps in solving optimization problems that are complex, nonlinear and multi-variable. Indeed, solving optimization problems became an important field of research during the last years because of its wide application in different fields such as management and engineering sciences.

Recently, new optimization theory and algorithms have been proposed by researchers based on new stochastic optimization methods, intelligent algorithms, heuristic and meta-heuristic algorithms such as: bee algorithm, ant colony and the genetic algorithms. However, each one among these algorithms has its appropriate application scope and limitations [36].

In this Chapter, the selected optimization methods for solving the OPP problem are presented in detail. These methods are the Particle Swarm Optimization (PSO), the Grey Wolf Optimizer (GWO), the Moth-flame Optimization (MFO), the Cuckoo search (CS) and the Wind Driven Optimization (WDO).It is to note here that the WDO is a heuristic method whereas the other methods are meta-heuristic, it has been selected in the goal to compare the behaviour of a heuristic method with the other meta-heuristic methods.

3.2 Basic concepts of the optimization problem

The main fundamental common concepts used in optimization problem are based on the following keystone elements:

a. **The objective function:** It expresses the main purpose of the model which is either to be minimized or maximized. It is also named as the optimization criterion, the cost function and the fitness function. Based on the objective function, two problem types can be distinguished:
   - Mono-objective function problem: an optimization problem with single objective function to be optimized.
   - Multi-objective function problem: an optimization problem with several objective

functions to be optimized simultaneously.

b. Variables: They are presented by a set of unknowns, which control the value of the objective function. They are adjusted iteratively during the optimization process, to obtain optimal solutions. They are also known as design variables or project variables.

c. Constraints: They are presented by a set of conditions, which allow the variables to take a certain values and to exclude others. By other words, the constraints present the conditions, which the variables must satisfy. These constraints can be inequality, equality or side constraints.

Solving an optimization problem is then can be defined as: finding a values of the variables that minimize or maximize the objective function while satisfying the constraints.

3.3 General optimization problem statement

A constrained optimization problem can be modelled as follows:

$$min\ (F(X)) \text{ or } max\ (F(X)) \tag{3.1}$$

Subject to:

Inequality constrains: $G_j(X) \geq 0 \quad or \quad G_j(X) \leq 0 \qquad j = 1, m$ (3.2)

Equality constrains: $H_k(X) = 0 \qquad k = 1, l$ (3.3)

Side constrains: $X_i^L \leq X_i \leq X_i^U \qquad i = 1, n$ (3.4)

Where $F(X)$ is the objective function and X is vector of design variables.

$$X = \begin{bmatrix} X_1 \\ X_2 \\ \vdots \\ \vdots \\ X_n \end{bmatrix} \tag{3.5}$$

3.4 Particle Swarm Optimization (PSO)

A particle swarm optimizer (PSO) is a population-based stochastic optimization algorithm modeled after the simulation of the social behavior of bird flocks and fish schooling. It is introduced firstly by James Kennedy & C.Eberhart in 1995, it has been successfully applied to a wide range of optimization problems of both continuous nonlinear and discrete optimization problems such as: Neural Networks, Shape topology and electric power distribution networks. [36]

3.4.1 How the particle swarm optimization works

A particle Swarm Optimization is a swarm intelligence method for a global optimization. In PSO a population (called swarm) fly through the search space. This swarm is a group of

individuals called particles that are looking for the best location. Each particle represents a candidate solution to the optimization problem, it adjusts its trajectory toward both of its own previous best position and the previous best position attained by any member of its topological neighborhood. So the position of a particle is influenced by the best position visited by itself and the position of the best particle in its neighborhood, when the neighborhood of a particle is the entire swarm. The best position achieved by each particle is referred to as local best position ($X_iBest - the\ best\ position\ of\ particle\ i$) while the best position in the entire swarm is referred to as the global best position (X_gBest). Each individual has a fitness function where the objective function is the global function whose maximum or minimum should be found. The fallowing sketched diagram clarifies the particle trajectory:

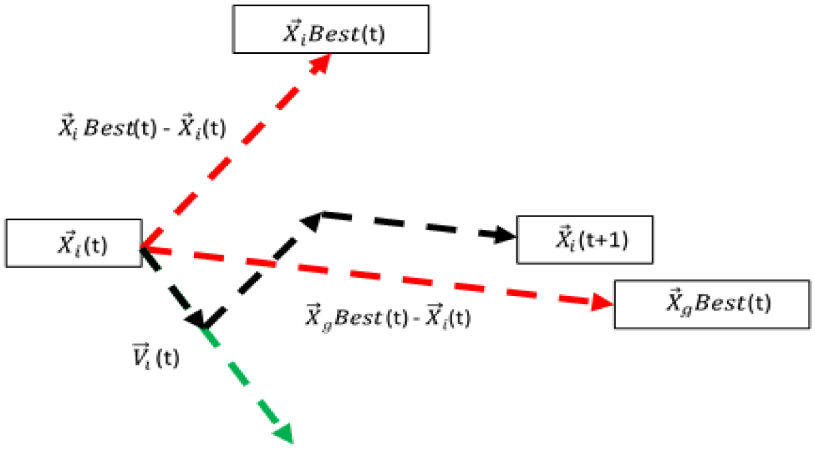

Figure 3.1. *Particle trajectory for PSO*

So each particle in the swarm is defined by the following characteristics:
X_i : The current position of particle i.
V_i : The current velocity vector of particle i.
X_iBest : The personal best position vector achieved by particle i or simply best "remembered" individual particle position.
X_gBest: The global best position vector for all the particles of the swarm or simply the best "remembered" swarm position.
All of this characteristics are multi-dimensional with the same dimension. It can be presented as follows:

$$X_i = [X_{i,1}, X_{i,2}, \dots\dots, X_{i,n}]$$
$$V_i = [V_{i,1}, V_{i,2}, \dots\dots, V_{i,n}] \quad (3.6)$$
$$X_iBest = [X_{i,1}Best, X_{i,2}Best, \dots\dots, X_{i,n}Best]$$

Where *n* is the number of variables in the fitness function.

In each step of time t (iteration) each particle updates its own position as follow:

$$X_i(t+1) = X_i(t) + V_i(t) \quad (2.7)$$

On the other side, the velocity is updated as follows:

$$V_i(t+1) = V_i(t) + \left(c_1 \times r_1 \times \left(X_iBest - X_i(t)\right)\right) + \left(c_2 \times r_2 \times \left(X_gBest - X_i(t)\right)\right) \quad (3.8)$$

Where:

$X_i(t+1)$: is the new position for the particle i at time step $(t+1)$.

$V_i(t+1)$: is the new velocity for the particle $i$at time step $(t+1)$.

r_2, r_1 : random values between 0 and 1.

c_1, c_2: cognitive and social parameters.

$X_iBest, X_gBest, V_i(t),\ X_i(t)$: as stated before.

Let $F(X)$ be the objective function, then the personal best position of a particle updates its self at time step t is as follows:

$$X_iBest\ (t+1) = \begin{cases} X_iBest(t) & F\left(X_iBest(t)\right) < F\left(X_iBest(t+1)\right) \\ X_iBest(t+1) & F\left(X_iBest(t+1)\right) < F\left(X_iBest(t)\right) \end{cases} \quad (3.9)$$

Simultaneously, the global best position is determined by selecting the personal best position of all particles at time step t, then the global best position is the personal best position in which the objective function has to be minimum or maximum. So X_gBest is included in the fallowing set:

$$X_gBest \in \left\{X_1Best\ , X_2Best, \dots\dots\dots, X_pBest\right\} \quad (3.10)$$

and it satisfies:

$$\begin{aligned} & F(X_gBest) = min\left\{F(X_1Best), F(X_2Best), \dots\dots\dots, F(X_pBest)\right\} \\ Or, \quad & F(X_gBest) = max\left\{F(X_1Best), F(X_2Best), \dots\dots\dots, F(X_pBest)\right\} \end{aligned} \quad (3.11)$$

All of the previous steps are repeated until a specific number of iteration (maximum number of iteration) is reached, or velocity updates becomes too close to zero. And the optimality of particles can be evaluated through how much the objective function tends to zero (in case if we are looking to find the minimum of the objective function) [37].The Pseudo code of PSO algorithm is presented in **Appendix A.1**

3.5 Grey Wolf Optimizer (GWO)

In 2014, S.Mirjalili introduced a new powerful meta-heuristic optimization algorithm known as the Grey Wolf Optimizer [38].This algorithm is inspired from the behavior of the Grey Wolf that belongs to “Canidae family”.

Grey wolf mostly prefers living in a pack of 5 to 12 maximum under strict social dominant hierarchy, the social hierarchy consists of four (04) levels as shown in Figure 3.2.The pack should follow the orders of the dominant wolf. The leader that can be male or female is known as Alpha (α), it is responsible for making decisions about time to walk, place where they are sleeping, hunting…etc. The Alpha wolf is the dominant wolf in all the pack and all his/her orders should be obeyed by the pack members. The Betas (β) are subordinate wolves which

help the alpha in decision making. The Beta wolf is considered to be the best candidate to take the place of the Alpha wolf in case of the Alpha becomes very old or passes away. Also, the Beta disciplines the pack and work as an advisor to Alpha. The Delta (δ) wolves submit to Alpha and Beta wolves but they dominate the Omega (ω), there are different categories of Delta wolves such as Scouts, Sentinels, Elders, Hunters and Caretakers. The Omega wolves are in the lowest level of social hierarchy, they are considered to be the scapegoat in the pack and they have to submit to all the other wolves. It seems that the Omega wolves are not important individuals in the pack and they are the last allowed wolves to eat.

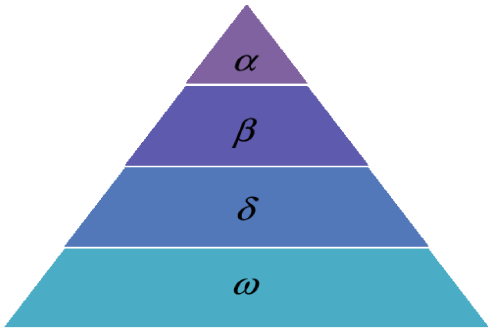

***Figure 3.2**. Hierarchy of grey wolf (dominance decreases from top down) [38].*

3.5.1 How the Grey wolf optimizer works

The main acts of grey wolf hunting are encircling, hunting and attacking the prey. The fittest solution is considered to be Alpha, and the second and third solutions are Beta and Delta, respectively. The other remaining solutions are considered to be Omega. The hunting is guided by α, β and δ. The other solutions (ω) follow these three wolves.

The mathematical model of the encircling behaviour is presented as follows:

$$\vec{D} = \left|\vec{C}.\vec{X}_{prey}(t) - \vec{X}_{wolf}(t)\right| \\ \vec{X}_{wolf}(t+1) = \vec{X}_{prey}(t) - \vec{A}.\vec{D} \tag{3.12}$$

Where t indicates the current iteration, $\vec{X}_{prey}(t)$ is the prey position vector, $\vec{X}_{wolf}(t)$is the grey wolf position vector,$\vec{D}$and $\vec{C}$are coefficient vectors calculated as follows:

$$\vec{A} = 2\vec{a}\overrightarrow{r_1} - \vec{a} \\ \vec{C} = 2\,\overrightarrow{r_2} \tag{3.13}$$

Where the entries of $\vec{a}$ are linearly decreased from 2 to 0 over the number of iterations, and $\overrightarrow{r_1}$ and $\overrightarrow{r_2}$are random vectors of entries varying within the interval of [0, 1]. Thus, by using equations (3.12) a grey wolf can update its position around the prey at any random location.

In modelling the hunting process of grey wolves, it is supposed that the Alpha wolf presents the best candidate solution. In addition to that the Beta and Delta wolves have better

information about the prey potential location. Therefore, the three best solutions obtained till the actual iteration are memorized to force the other search candidates to update their positions. Figure 3.3 shows how a wolf updates its position in a 2D search space.

The position vector of all the wolves can be updated with respect to Alpha, Beta and Delta as follows:

$$\begin{aligned} \overrightarrow{D_\alpha} &= \left|\overrightarrow{C_1 X_\alpha}(t) - \overrightarrow{X_{wolf}}(t)\right|, \quad & \vec{X}_1 &= \vec{X}_\alpha(t) - \overrightarrow{A_1}.\overrightarrow{D_\alpha} \\ \overrightarrow{D_\beta} &= \left|\overrightarrow{C_2 X_\beta}(t) - \overrightarrow{X_{wolf}}(t)\right|, \quad & \vec{X}_2 &= \vec{X}_\beta(t) - \overrightarrow{A_2}.\overrightarrow{D_\beta} \\ \overrightarrow{D_\delta} &= \left|\overrightarrow{C_3 X_\delta}(t) - \overrightarrow{X_{wolf}}(t)\right|, \quad & \vec{X}_3 &= \vec{X}_\delta(t) - \overrightarrow{A_3}.\overrightarrow{D_\delta} \end{aligned} \tag{3.14}$$

The best position which can be taken by a wolf can be calculated as the average, hence it is expressed as follows:

$$\overrightarrow{X_{wolf}}(t+1) = \frac{\vec{X}_1 + \vec{X}_2 + \vec{X}_3}{3} \tag{3.15}$$

All of the previous steps are repeated until a maximum number of iterations are reached.

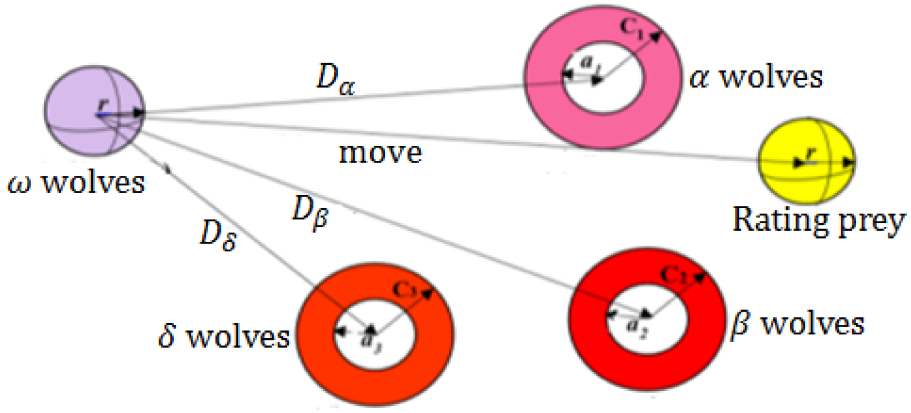

Figure 3.3. *Position updating in GWO*

The Pseudo code of GWO algorithm is presented in **Appendix A.1**

3.6 Moth Flam Optimization (MFO)

Moth-flame optimization algorithm (MFO) is a new meta-heuristic optimization algorithm introduced by S.Mirjalili in 2015, this algorithm mimics the motion of moths' flight around the flames. The natural moth navigation method is known as transverse orientation. In this method, a moth flies by keeping a fixed angle with the moon, this method shows a very effective technique for travelling in a straight path because the moon is very far away from the moth. However, when the light source (for example, flame or human-made artificial light) is close, moths try to keep a fixed angle with the light to fly in straight line but moths fly spirally around it and finally converge toward it since it is extremely close compared to the moon [39-41].

3.6.1 How the moth flam optimization works

Moths and flames are the key components in the MFO algorithm, the moth is the actual search body moving in the search space while the flames are the best solution achieved by the search bodies so far and they are updated in case of finding better solution. The set of moths and their corresponding fitness values are represented in matrices as follows:

$$M = \begin{bmatrix} m_{1,1} m_{1,2} \dots m_{1,d} \\ m_{2,1} m_{2,2} \dots m_{2,d} \\ \vdots \quad \vdots \quad \vdots \quad \vdots \\ m_{n,1} m_{n,2} \dots m_{n,d} \end{bmatrix}, OM = \begin{bmatrix} OM_1 \\ OM_2 \\ \vdots \\ OM_n \end{bmatrix} \tag{3.16}$$

where n and d are the number of moths and variables respectively, also the flames and their fitness values are represented initially in matrices similar to the moth matrices as follows:

$$F = \begin{bmatrix} F_{1,1} F_{1,2} \dots F_{1,d} \\ F_{2,1} F_{2,2} \cdots F_{2,d} \\ \vdots \quad \vdots \quad \vdots \quad \vdots \\ F_{n,1} F_{n,2} \cdots F_{n,d} \end{bmatrix}, OF = \begin{bmatrix} OF_1 \\ OF_2 \\ \vdots \\ OF_n \end{bmatrix} \tag{3.17}$$

The transverse orientation can be model mathematically through the logarithmic spiral, hence the position of each moth is updated with respect to a flame using the following equation:

$$M_i = D_i . e^{bt} \cos(2\pi t) + F_j \ , \ D_i = \left| F_j - M_i \right| \tag{3.18}$$

Where M_i is the i^{th} moth, F_j is the j^{th} flame, D_i means the Euclidian distance between the i^{th} moth and the j^{th} flame, b is a constant that defines the logarithmic spiral shape and t is a random number in the interval of [−1, 1]. The t parameter specifies how close is the next moth position to the flame as shown in Figure 3.4. To emphasize exploitation, t is taken as a random number in the interval [r,1] where r decreases linearly from −1 to −2 during iterations, r is known as convergence constant.

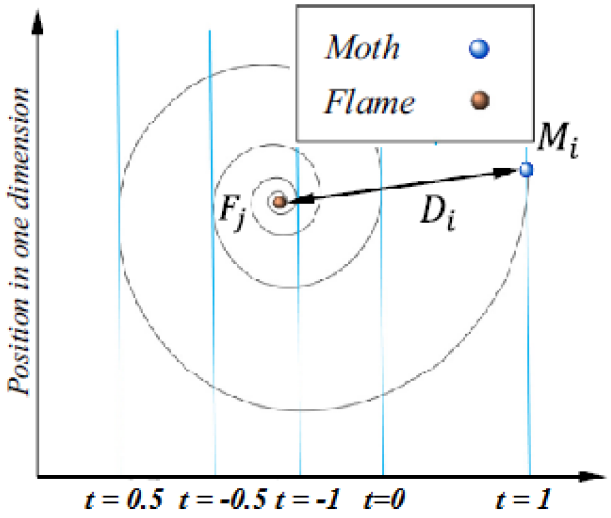

Figure 3.4. *Logarithmic spiral, the positions of moth around a flame with respect to t [39].*

In each iteration, the list of flames are updated and sorted based on the fitness values. Then, the moths update their positions toward their flames. The first moth is always updating its position to the best flame while the last moth to the worst flame of the list. Another problem here is that the position updating of moths to *n* different locations may degrade the exploitation of the best promising solutions, thus the number of flames to be followed is reduced during iterations as shown in the following expression:

$$number\ of\ flames = \left(N - l \times \frac{N-1}{T}\right) \tag{3.19}$$

Where *N* is the number of moths, *l* is the number of current iteration and *T* is the number of iterations. Once the maximum iteration is reached, the best moth is returned as the best approximation of the optimum. The Pseudo code of MFO algorithm is presented in **Appendix A.2**

3.7 Cuckoo Search (CS) via Lévy flights

Cuckoo search (CS) is one of the natured-inspired meta-heuristic algorithms, it has been developed in 2009 by Xin-she Yang and Suash Deb. The cuckoo search is based on the brood parasitism of certain cuckoo species. These species lay their eggs in the nests of other host birds (other species), if a host bird discovers the eggs are not their own, it will either throw these eggs away or simply abandon its nest and build a new nest elsewhere. This algorithms is improved by the well-known Lévy flights. The Lévy flights are random walks whose step length is drawn from the Lévy distribution, Figure 3.5 shows Lévy flights path of 50 steps with starting point (0,0).[42-43]

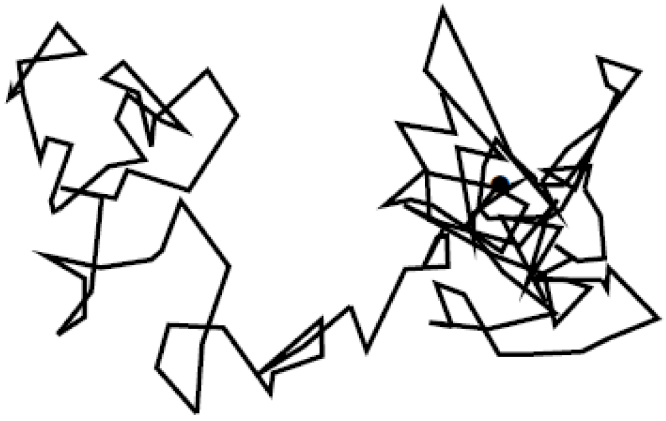

Figure 3.5. *Lévy flights path of 50 steps in 2D (β=1) [43].*

3.7.1 How the cuckoo search via lévy flights works

The CS is based on three idealized rules:

- Each cuckoo lays one egg at a time, and dumps its egg in a randomly selected nest.

- The best nests (with high-quality eggs) will be carried over to the next generations;
- The number of available host nest is fixed. In case of discovering an alien egg by the host, the host bird can either throw the egg away or abandon the nest to build another one elsewhere. This assumption can be approximated as the probability of discovering an alien egg by the host is greater than P_a, the host nest are replaced by new nest.

In simplest form, each nest has one egg, and each egg in a nest represents a solution $X_i(t)$ while a cuckoo egg represents a new solution. The goal is to use new and better solutions (cuckoos) to replace a less-good solutions by looking for other good nests instead of less-good nest. A lévy flight is performed when generating new solution $X(t+1)$ for a cuckoo i as follows:

$$X_i(t+1) = X_i(t) + \alpha . Lévystep(\beta) \tag{3.20}$$

Where α> 0 is the step size.

Generating random numbers with Levy flights consists of two steps: selecting a random **direction** and generating **steps**, which obey the lévy distribution. For the generation of a direction a uniform distribution should be used, hence [43]:

$$Lévystep(\beta) = s(\beta).randn(size(X_i(t))) \tag{3.21}$$

Where s is the step length and β taken to be 1.5. The operator (.) is an entry wise multiplication. For the generation of steps the so-called Mantegna algorithm is used as follows [43]:

$$s = \frac{U}{|V|^{-\beta}} \tag{3.22}$$

Where

$$U \sim N(0, \sigma_u^2)\,, \quad V \sim N(0, \sigma_v^2) \tag{3.23}$$

$$\sigma_u = \frac{\Gamma(1+\beta)\sin(\pi\beta/2)}{\Gamma[(1+\beta)/2]\,\beta 2^{(\beta-1)/2}} \quad , \quad \sigma_v = 1 \tag{3.24}$$

After that the good nest will be carried according to the fitness value as follows (case of minimum objective function):

$$X_i(t+1) = \begin{cases} X_i(t) & F\big(X_i(t)\big) < F\big(X_i(t+1)\big) \\ X_i(t+1) & F\big(X_i(t+1)\big) < F\big(X_i(t)\big) \end{cases} \tag{3.25}$$

Or any other nest j can be chosen randomly and updated as follows:

$$X_j(t+1) = \begin{cases} X_j(t) & F\left(X_j(t)\right) < F\big(X_i(t+1)\big) \\ X_i(t+1) & F\big(X_i(t+1)\big) < F\left(X_j(t)\right) \end{cases} \tag{3.26}$$

Now, according to the third rule, if the probability of discovering an alien egg by the host is greater than P_a, the host nest is replaced by new nest elsewhere. So, in each iteration, each coordinate of each nest is assigned randomly with probability value. If it exceeds ($P_a = 0.25$), it will be changed, thus the nest will be replaced. In nature, if a cuckoo's egg is similar to a host's eggs, then this cuckoo's egg is less likely to be discovered by the host, hence the fitness should be related to the difference in solutions. Thus, it is a good idea to do a random walk in

a biased way with some random step sizes. So, in this case, the nest will be replaced as follows:

$$X_i(t+1) = X_i(t) + rand.\left(X_j(t) - X_z(t)\right).K \quad (3.27)$$

Where j and z indicate nests chosen randomly and by permutation, and K is a vector that indicates the coordinates that should be replaced, its entries either by 1 or 0. Again, the good nest will be carried according to the fitness value as shown in Equation (3.25).

All of the previous steps are repeated until the maximum iteration is reached then the best nest among the available nests is returned as the best approximation of the optimum.

The Pseudo code of CS algorithm is presented in **Appendix A.2.** It is worthy to mention that the generation of new solutions may use slightly different methods.

3.8 Wind Driven Optimization (WDO)

The Wind-Driven Optimization (WDO) is a population based iterative heuristic global optimization technique. It is developed in 2010 by Zikri Bayraktar [44-45].The inspiration of this algorithm comes from atmospheric motion in which the infinitesimally small air parcel trajectory can be modelled via Newton's second law of motion, where the wind blows in order to equalize horizontal imbalances in the air pressure, it blows from a high pressure to low pressure region at a velocity proportional to the pressure gradient ∇P which can be defined as the pressure change across a given distance [46].

3.8.1 How the wind driven optimization works

Mainly, there are four forces, which cause the wind to move at a certain speed in a certain direction or deflect it from its current path:

- Pressure gradient force ($\boldsymbol{F_{PG}}$): the most observed force that causes the air to move, it comes as a result of variations in air pressure at different locations. Given the fact that the air has finite mass and volume (δV), F_{PG} can be expressed as shown in Equation (3.28).
- Gravitational force ($\boldsymbol{F_G}$): is an attractive force that pulls the air parcels towards the origin of the coordinate system.
- Friction force ($\boldsymbol{F_F}$): acts to oppose the motion, it can be simplified as described in equation (3.28).
- Coriolis force ($\boldsymbol{F_C}$): is caused by the rotation of the earth, and deflects the path of the wind from its existing path. In WDO, This force is implemented as a motion in a dimension affecting velocity in other different dimension i.e. the motion in a specific dimension will be influenced by the motion in another randomly selected dimension at each iteration.

$$\overrightarrow{F_{PG}} = -\nabla P \ \delta V;\ \overrightarrow{F_g} = \rho\ \delta V\ g;\ \overrightarrow{F_F} = -\rho\ \alpha\ U;\ \overrightarrow{F_C} = -2\Omega \times U \quad (3.28)$$

where ∇P is the pressure gradient, δV an infinitesimal air volume, ρ is the air density for an infinitesimal small air parcel, g is the gravitational acceleration, α is the friction coefficient,U is the velocity vector of the wind and Ω represents the earth rotation vector. The relation between the air pressure and its density and temperature is described by the ideal gas law as follows:

$$P_{cur} = \rho\, R\, T \tag{3.29}$$

Where P is the current pressure, T is the temperature and R is the universal gas constant.

Substituting the previously described forces in Newton's second law of motion leads to:

$$\rho \frac{\Delta U}{\Delta t} = (\rho\, \delta V\, g) + (-\rho\, \alpha\ U) + (-\nabla P\ \ \delta V) + (-2\Omega \times U) \tag{3.30}$$

For simplicity, time step Δt is assumed to be 1 and for dimensionless and small infinitesimal air parcel δV is set to be 1. Also, dividing both sides of equation (3.30) by ρ and substituting ρ by P_{cur}/RT from Equation (3.29) results in:

$$\Delta U = g - \ \alpha\ U + \left(-\nabla P\ \ \frac{RT}{P_{cur}}\right) + \frac{(-2\Omega \times U)RT}{P_{cur}} \tag{3.31}$$

The change in velocity can be expressed as:

$$\Delta U = U_{new} - U_{cur} \tag{3.32}$$

Where U_{cur} the current iteration velocity and U_{new} is the next iteration velocity.

Since the gravitational force pulls an air parcel from its current location towards the origin of the system, the term g can be expressed as follows:

$$g = |g|(0 - X_{cur}) \tag{3.33}$$

The pressure gradient is defined as the force that moves the air parcel from its current location to an optimal pressure point. Hence, the pressure gradient is directed from the current location X_{cur} of an air parcel to the optimum location X_{opt} found so far by the population, and the magnitude is the pressure difference between the current location P_{cur} and the optimum location P_{opt}. Therefore, the pressure gradient can be written as follows:

$$-\nabla P = \left|P_{opt} - P_{cur}\right|\left(X_{opt} - X_{cur}\right) \tag{3.34}$$

where the minus sign indicates the descending direction in the gradient.

As mentioned previously, the effect of the Coriolis force is replaced by the velocity influence from another randomly chosen dimension of the same air parcel $U_{cur}^{other\ dim}$, thus the Coriolis force can be simplified as follows:

$$\overrightarrow{F_C} = -2\Omega \times U = -2|\Omega|U_{cur}^{other\ dim} \tag{3.35}$$

Taking $C = -2|\Omega|RT$, and substituting (3.32),(3.33),(3.34) and (3.35) in (3.31) results in:

$$U_{new} = (1-\alpha)U_{cur} - gX_{cur} + \left(\left|P_{opt} - P_{cur}\right|\left(X_{opt} - X_{cur}\right)\frac{RT}{P_{cur}}\right) + \frac{C.U_{cur}^{other\ dim}}{P_{cur}} \quad (3.36)$$

The problem in equation (3.36) is that the pressure values are explicitly used, so to overcome this problem, a ranking approach may be used in which the population of air parcels is classified in decreasing order based on their pressure values (fitness values). Thus, Equations (3.36) can be written as shown below where *i* is the ranking among all air parcels. For example the best solution X_{opt} has the rank 1 because it has the lowest pressure (fitness value).

$$U_{new} = (1-\alpha)U_{cur} - gX_{cur} + \left(\left|\frac{1}{i} - 1\right|\left(X_{opt} - X_{cur}\right)\frac{RT}{P_{cur}}\right) + \frac{C.U_{cur}^{other\ dim}}{i} \quad (3.37)$$

Once the new velocity is calculated, the position of the air parcel can be updated by the following equation:

$$X_{new} = X_{cur} + U_{new} \quad (3.38)$$

It should be noted that the new velocity of each air parcel is limited to a maximum value per iteration to prevent taking large steps and overlooking certain regions in the search space. So:

$$U_{new} = \begin{cases} U_{max} & U_{new} > U_{max} \\ -U_{max} & U_{new} < -U_{max} \end{cases} \quad (3.39)$$

In WDO algorithm, a population of air parcels are initialized with random positions and velocities. Using Equations (3.37) and (3.38), the air parcels update their positions and velocities in each iteration toward the found optimum pressure location so far, taking into account the limitation mentioned in Equation (3.39). At the end of the last iteration, the optimum solution will be obtained. The Pseudo code of the WDO algorithm is presented in **Appendix A.3**. In the implementation of the WDO algorithm the parameters in Equation (3.37) have been taken to be as follows: RT = 3, g = 0.2, α = 0.4, C = 0.4 and U_{max} = 0.3.

3.9 Conclusion

This chapter elaborates the basic concept and operation of the selected optimization algorithms, and the main idea of their implementation. In addition, the Pseudo codes of each algorithm are presented in **Appendix A**, which will be used in the next chapter for solving the OPP problem for different selected power systems.

CHAPTER 4

Application to Power Networks

- *Introduction*
- *Optimization problem conditions*
- *Results and discussions*
- *Conclusion*

Application to Power Networks

4.1 Introduction

The proposed methods are applied to solve the OPP problem for various IEEE bus systems ranging from 9-bus until 30-bus systems in addition to the Algerian grid system of 114 buses. The one line diagram for each system is shown in **Appendixes**. The algorithms are implemented using MATLAB R2016a software, the technical specifications of the computer used to perform the algorithms are Intel core i5, 2.6 GHz and 6 GB of RAM.

The proposed OPP formulation is solved employing the aforementioned optimizations techniques (PSO, GWO, MFO, CS and WDO) by considering two cases. The considered cases are as the following:

- Ignoring ZIBs (Normal operation)
- Considering ZIBs

As a result for this application, the number of PMUs required for each system tested, including its locations, and the SORI value for each set of PMUs are given.

4.2 Optimization problem conditions

The main goal is to use the proposed algorithms to determine the minimum number of PMUs, which allow ensuring the full observability. Hence, each algorithm should find its best possible solution that can achieve the main objective regarding to the constraint. The fitness function that represents the main objective is used for the evaluation of every possible solution acquired by the particles, also used to differentiate the quality of each particle solution, where a decision can be made about which candidate is the best solution for the problem. The objective function and the constraint are re-presented in the following subsections in addition to the simulation parameters.

4.2.1 The objective function

The objective function is to find the minimum number of PMUs that maintains the full observability of the system while maximizing system observability redundancy index (SORI). This can be presented by the previous discussed equations (2.15) and (2.23). The applied algorithms are heuristic and meta-heuristic algorithms, so multiple solutions are expected. To differentiate the quality of each solution among the other solutions, which have the same number of PMUs, the solution that has the highest SORI value will be selected as the best optimal solution. Since the implemented objective function is mono-objective function that

achieves the minimization of the number of PMUs. The possible solution of each iteration corresponding to the minimum number of PMUs is recorded, and then the one with the highest SORI will be selected as an optimal solution.

4.2.2 The constraints

In our case, the constraint is the modelled part that ensures the observability of the whole system by ensuring the observability of each bus alone. Hence, the constraint can be presented as a vector that has a dimension equal to the number of buses. Whereas in the case of considering the ZIBs, this vector will be have a dimension which is equal to the number of buses without the ZIBs. This vector is called constraint vector function, its formulation is explained in detail in the second Chapter in both cases of ignoring and considering the ZIBs.

4.2.3 The parameters of the algorithms

The parameters of the applied algorithms are presented in the flowing Table:

Table 4.1*. Algorithms' parameters*

The parameters	**PSO**	**GWO**	**MFO**	**SC**	**WDO**
Population Size	200	200	200	200	200
Maximum number of iterations/generations	Highest number of iterations to ensure that the algorithms reach its minimum solution				

4.3 Results and discussions

The application of the optimization methods Particle Swarm Optimization (PSO), Grey Wolf Optimizer (GWO), Moth-flame Optimization (MFO), Cuckoo search (CS) and Wind Driven Optimization (WDO) are investigated on the following selected power networks in both cases of ignoring and considering the ZIBs where the implementation of these proposed algorithms is done using MATLAB software:

- IEEE 09-bus system
- IEEE 14-bus system
- IEEE 30-bus system
- Algerian grid 114-bus system

4.3.1 IEEE 09-bus system

As the name suggests, the IEEE 9-bus system consists of 9 buses in total and there are 3 zero-injection buses. This test case also includes three transformers, 6 transmission lines and 3 loads. The single line diagram of this system is depicted in **Appendix B**. The information related to the structure and connectivity of the 9-bus system is provided in Table 4.2.

***Table 4.2**. Data about the IEEE 9-bus system*

System	Number of branches	Number of zero injection buses	Location of zero injection buses
IEEE 9-bus	9	3	4 6 8

4.3.1.1 Case of ignoring ZIBs

In this case, the OPP problem is solved by ignoring ZIBs. The number of PMUs required for IEEE 9-bus system including their locations and the SORI value for each PMUs placement set are given in Table 4.3. Also, the objective function graph for each optimization method is depicted in Figure 4.1.

***Table 4.3.** Optimal PMUs placement results for IEEE 9-bus system without considering ZIBs*

Methods	Number of PMUs	Positions	SORI
PSO	3	3 4 8	10
GWO	3	4 6 8	12
MFO	3	4 6 8	12
CS	3	3 4 8	10
WDO	3	4 6 8	12

According to the results presented in Table 4.3, the achieved minimum number of PMUs is 3 through all the applied algorithms. Obviously, there is no unique solution that is why different PMUs placement sets are found, hence different values of SORI. The PMUs located at 3, 4 and 8 buses achieves SORI of 10. However, PMUs located at 4, 6 and 8 buses achieves SORI of 12, it is worthy to note that many PMUs placement sets may have the same SORI value. For comparison, the same result of minimum number of PMUs has been obtained in [47].

In terms of iterations, according to the results presented in Figure 4.1, it is clear that the algorithms of PSO, GWO and WDO converge to their final minimum value at the second iteration, while MFO and CS converge at their final minimum at the third iteration.

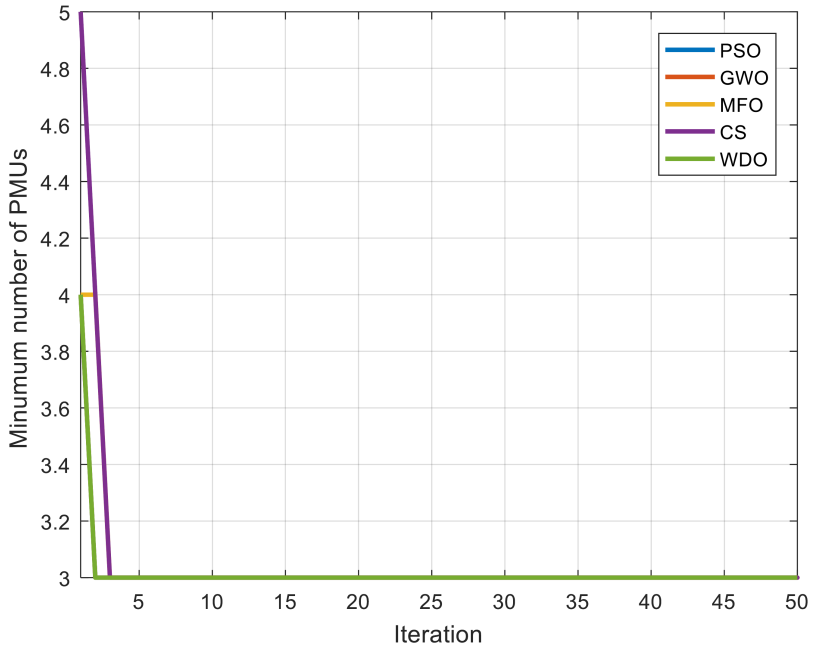

Figure 4.1. *The objective function graphs for the OPP problem of the IEEE 9-bus system when ignoring ZIBs*

4.3.1.2 Case of considering ZIBs

In this case, the presence of ZIBs in power system is considered when solving the OPP problem. The ZIBs locations for IEEE 9-bus system are given in Table 4.2. Meanwhile, the obtained results for this system are given in Table 4.4. Whereas, the objective function graph for each optimization technique are shown in Figure 4.2.

Table 4.4*. Optimal PMUs placement results for IEEE 9-bus system when considering ZIBs*

Methods	Number of PMUs	Positions	SORI
PSO	2	6 8	8
GWO	2	4 6	8
MFO	2	4 6	8
CS	2	6 8	8
WDO	2	4 8	8

According to the obtained results of the case when ZIBs are considered, which are presented in Table 4.4, the achieved minimum number of PMUs by different applied algorithms is 2. It can be noted that the number of PMUs required is reduced by 1 when the presence of ZIBs in the power system are considered compared to the obtained results for normal operation. The obtained solution is not unique that is why different two PMUs placement sets are found. Hence the PMUs should be located either in 6 and 8 buses or in 4 and 6 buses to have full observability. For both solutions the value of SORI is the same.

According to the objective function graphs shown in Figure 4.2. The algorithms of WDO and GWO converge to their final value at the second iteration, the PSO algorithm reaches its minimum at the third iteration and the MFO reach its minimum at the fourth iteration. While the CS converges at the thirteenth iteration. So in terms of rapid convergence in the case of IEEE 9-bus system, the WDO and GWO methods are more effective compared to the other methods in the both cases of ignoring and considering ZIBs.

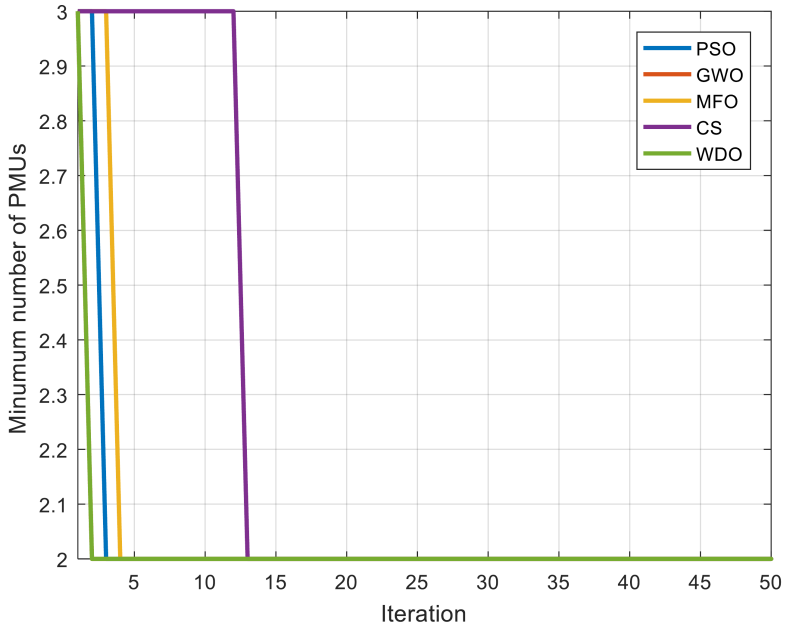

Figure 4.2. *The objective function graphs for the OPP problem of the IEEE 9-bus system when considering ZIBs*

4.3.2 IEEE 14-bus system

The IEEE 14-bus system contains only one zero-injection bus. Its single line diagram is depicted in **Appendix C**. The information related to the structure and connectivity of the IEEE 14-bus system is shown in Table 4.5.

Table 4.5. *Data about the IEEE 14-bus system*

System	Number of branches	Number of zero injection buses	Location of zero injection buses
IEEE 14-bus	20	1	7

4.3.2.1 Case of ignoring ZIBs

In this case, the OPP problem is solved by ignoring the ZIB located at bus number 7 and considered as a simple bus. The number of PMUs required for IEEE 14-bus system including their locations and the SORI value for each PMUs placement set are given in Table 4.6. In addition to that the objective function graphs for each optimization method are depicted in Figure 4.3.

Table 4.6. *Optimal PMUs placement results for IEEE 14-bus system without considering ZIBs*

Methods	Number of PMUs	Positions	SORI
PSO	04	2 6 7 9	19
GWO	04	2 6 7 9	19
MFO	04	2 6 7 9	19
CS	04	2 6 7 9	19
WDO	04	2 7 11 13	16

The results of all applied optimization methods show that the minimum number of PMUs that can be installed while maintaining the system full observable, is 4. The PMUs placement set found by all the algorithms except WDO is the same with SORI value of 19. While the placement set obtained by the WDO algorithm is of SORI value equals to 16. As a comparison with the reference [48], the same result achieved by all the algorithms has been obtained, except for WDO algorithm.

From Figure 4.3 which presents the objective function graphs in terms of iterations, it is found that The WDO algorithm converges firstly at the second iteration. Then PSO, MFO, GWO and CS algorithms converge at iteration number 5, 8, 17 and 44 respectively.

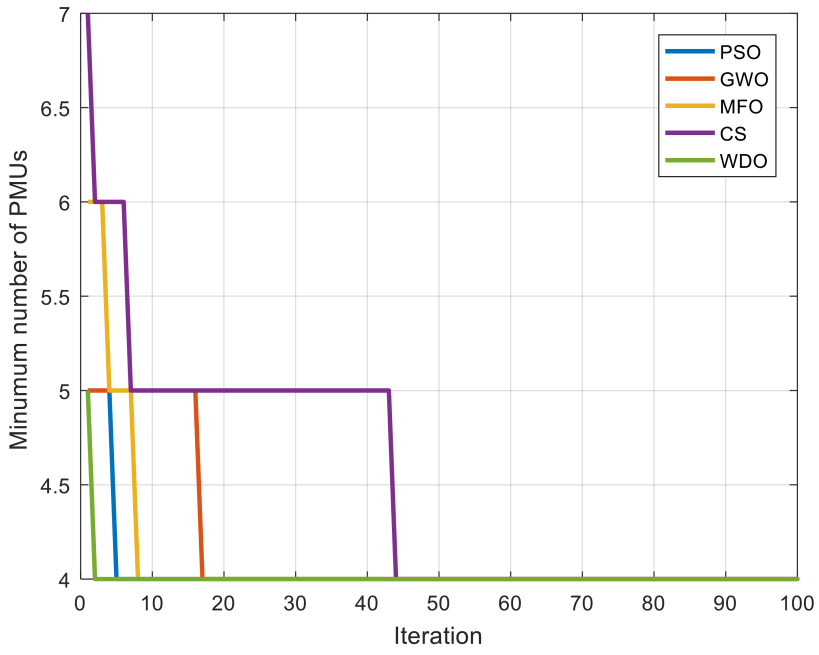

Figure 4.3. *The objective function graphs for the OPP problem of the IEEE 14-bus system when ignoring ZIBs*

4.3.2.2 Case of considering ZIBs

The presence of ZIB is considered when solving the OPP problem. The ZIB location is at bus 7. The results obtained are presented in Table 4.7. Whereas, the objective function graph for each optimization method is presented in Figure 4.4.

Table 4.7. *Optimal PMUs placement results for IEEE 14-bus system when considering ZIBs*

Methods	Number of PMUs	Positions	SORI
PSO	03	2 6 9	15
GWO	03	2 6 9	15
MFO	03	2 6 9	15
CS	03	2 6 9	15
WDO	03	2 6 9	15

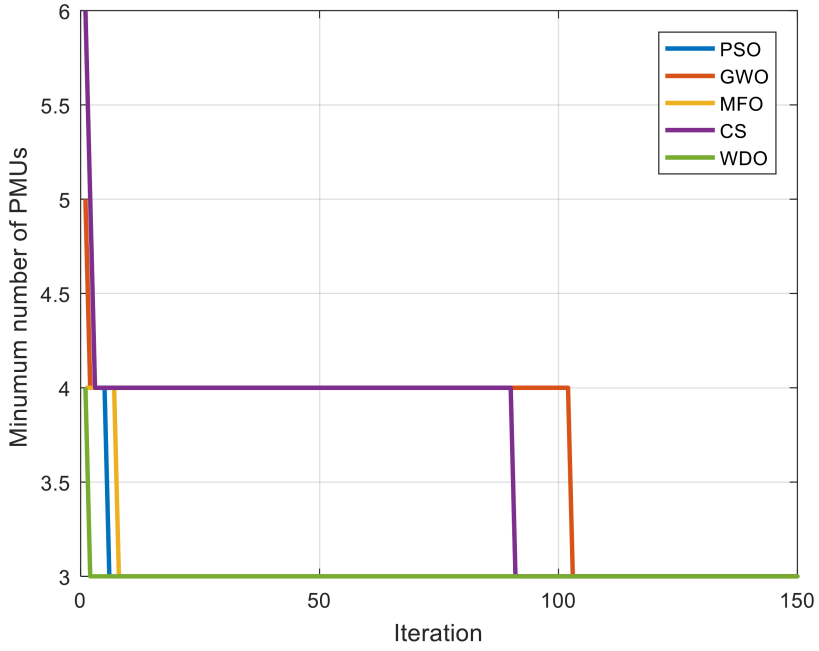

Figure 4.4. *The objective function graphs for the OPP problem of the IEEE 14-bus system when considering ZIBs*

Compared to the results obtained for normal operation, the number of PMUs required is reduced by one because of considering the presence of ZIB. The achieved minimum number of PMUs by all applied algorithms is 3. The resultant placement sets of all algorithms are identical with SORI value of 15.

According to the objective function graphs shown in Figure 4.3. The WDO as in the previous cases converges quickly to its final value, more precisely at the second iteration. The other algorithms converge differently starting from the sixth iteration (PSO) up to the iteration 103 (GWO). The same results has been also achieved in [48].

4.3.3 IEEE 30-bus system

The IEEE 30-bus system represents a simple approximation of the American Electric Power system as it was in December 1961 [49]. As shown in **Appendix D**, it has 6 zero-injection buses located at bus 6, 9, 22, 25, 27 and 28. Compared to the IEEE 14-bus system, this system is more complex, the total number of branches rising from 20 to 41. Information about the 30-bus system structure is given in Table 4.8.

Table 4.8. *Data about the IEEE 30-bus system*

System	Number of branches	Number of zero injection buses	Location of zero injection buses
IEEE 14-bus	41	6	5 6 9 11 25 28

4.3.3.1 Case of ignoring ZIBs

In this case, the algorithms are applied to solve the OPP problem by ignoring ZIBs. The number of PMUs required for IEEE 30-bus system including their locations and the SORI value for each PMUs placement set are presented in Table 4.9. Also, the objective function graph for all algorithms is depicted in Figure 4.5.

Table 4.9.*Optimal PMUs placement results for IEEE 30-bus system without considering ZIBs*

Methods	Number of PMU	Positions	SORI
PSO	10	1 5 6 9 10 12 15 19 25 27	48
GWO	10	3 6 7 9 10 12 15 18 25 27	48
MFO	10	1 6 7 9 10 12 15 20 25 29	46
CS	10	2 4 6 9 10 12 19 23 25 27	50
WDO	10	1 7 9 10 12 15 19 25 27 28	44

Based on the results presented in Table 4.9, the required minimum number of PMUs to achieve full observability is ten (10). Different PMUs placement sets are found by all algorithms. The solutions obtained by PSO and GWO have SORI value of 48, where WDO, MFO and CS have SORI values of 44, 46 and 50 respectively. Hence placement set acquired by the SC algorithm is the best among the other solutions because it has the highest value of SORI. In comparison with [48], the same result of minimum number of PMUs has been obtained.

From Figure 4.5 which represents the objective function graphs, The WDO algorithm converges firstly at the fourth iteration. Then GWO, MFO, CS and PSO algorithms converge at iteration number 24, 40, 53 and 114 respectively. It is clear to note here that all the algorithms

converge to the same minimum number of PMUs at different number of iterations with different placement sets and SORI values. It can be noticed that the WDO algorithm converges firstly but it doesn't provide the solution with highest value of SORI.

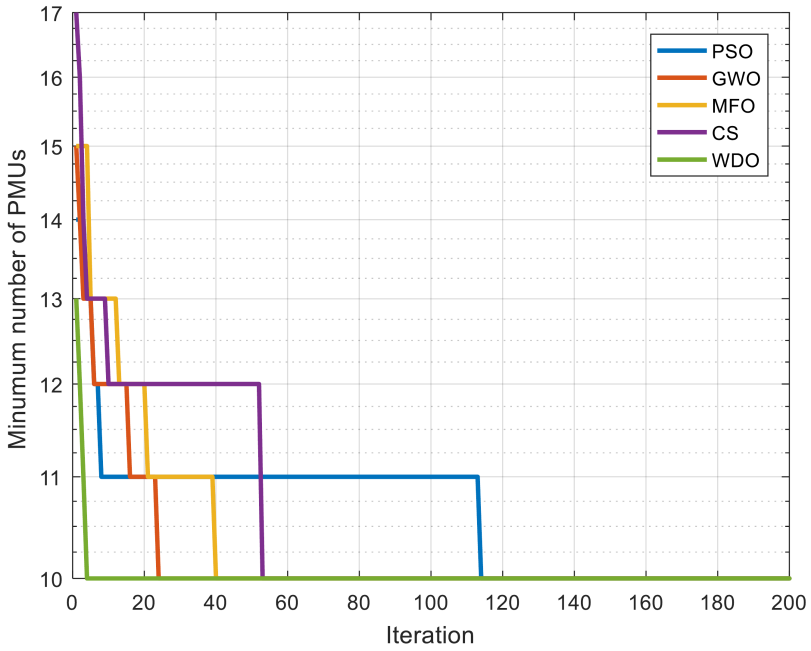

Figure 4.5. *The objective function graphs for the OPP problem of the IEEE 30-bus system when ignoring ZIBs*

4.3.3.2 Case of considering ZIBs

In this case, The ZIBs are considered when solving the OPP problem. The ZIBs locations for IEEE 30-bus system are given in Table 4.8. While the obtained results for this system are presented in Table 4.10 and the objective function graph for each optimization method are shown in Figure 4.6.

Table 4.10. *Optimal PMUs placement results for IEEE 30-bus system when considering ZIBs*

Methods	Number of PMUs	Positions	SORI
PSO	7	1 6 10 12 19 25 30	34
GWO	7	3 6 10 12 19 24 27	36
MFO	7	3 6 10 12 18 25 27	36
CS	7	1 6 10 12 18 25 27	36
WDO	8	3 6 12 19 22 24 25 27	37

The results presented in Table 4.10 show that the achieved minimum number of PMUs obtained by the application of the different algorithms is seven (07), except for the WDO algorithm where it achieves eight (08). So when the ZIBs are considered the number of PMUs required is reduced by three except the case of WDO which is reduced only by two. It can be

noticed here that as the problem complexity increases different results of minimum number of PMUs obtained, this can be explained by the capability of the optimization method used in finding the best solution in a specific application. SORI value of 37 is obtained by WDO algorithm but with 8 PMUs, where with 7 PMUs a value of 36 is acquired according to the result of GWO, MFO and CS. So it is preferred to select one of the placement sets provided by the three previously mentioned algorithms. The selected result is the same as obtained in [48]

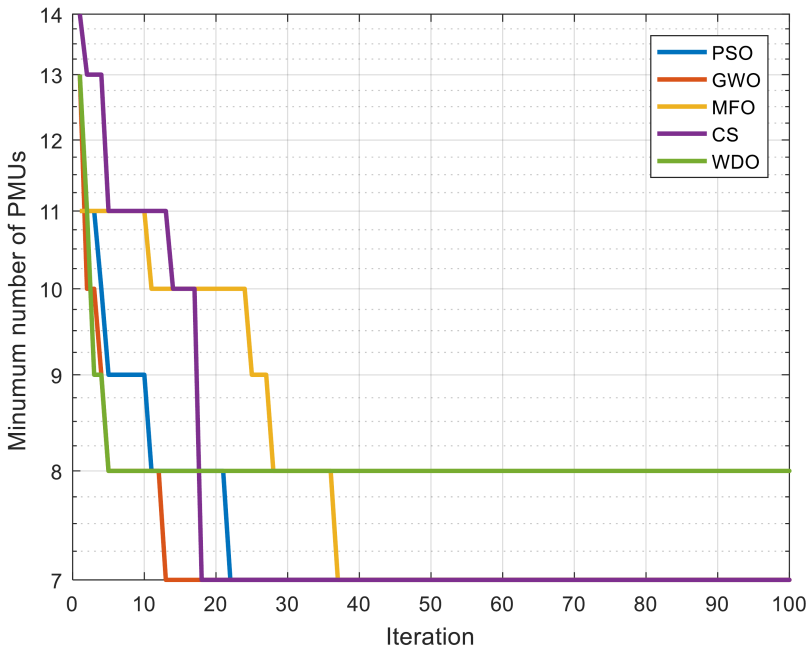

Figure 4.6. *The objective function graphs for the OPP problem of the IEEE 30-bus system when considering ZIBs*

In terms of iterations, from Figure 4.6, it can be seen that the WDO algorithm converges to its final value at the fifth iteration, the GWO reaches its minimum at 13th iteration, the CS reaches its minimum at iteration 18. While the PSO and MFO converge at their unique final value at iterations 22 and 37 respectively. It can be remarked that the WDO algorithm converges firstly compared to the other algorithms but it does not converge to the same minimum number of PMUs as the other algorithms. Hence, the GWO is the more effective algorithm in this case.

4.3.4 Algerian grid 114-bus system

The Algerian grid system consists of 175 transmission lines (branches), 15 generator-buses, 99 load-bus, and 17 tap changer transformers. Among the 114 buses there are 22 zero injection buses. Its connectivity data is presented in **Appendix E** [50].Compared to the IEEE 30-bus system, the complexity of this system increases dramatically, the total number of branches

rising from 41 to 175. The information related to the structure and connectivity of the Algerian grid 114-bus system are tabulated in Table 4.11:

Table 4.11. *Data about the Algerian grid 114-bus system*

System	Number of branches	Number of zero injection buses	Location of zero injection buses
Algerian grid 114-bus system	175	22	2 14 16 18 27 28 31 42 44 46 48 58 60 64 72 74 75 81 86 93 96 105

4.3.4.1 Case of ignoring ZIBs

In this case, the OPP problem is solved in normal operation where all the buses are considered as a simple buses. The number of PMUs required for Algerian network system including their locations and the SORI value for each PMUs placement set are presented in Table 4.12. Also, the objective function graph for each optimization method are shown in Figure 4.7.

Table 4.12. *Optimal PMUs placement results for the Algerian grid system without considering ZIBs*

Methods	**Number of PMUs**	**Positions**	**SORI**
PSO	44	1 3 4 11 12 14 16 17 18 19 22 23 26 29 36 38 41 44 46 47 52 55 57 61 65 67 71 75 76 78 82 87 88 90 93 95 99 100 105 108 109 110 112 113	180
GWO	38	1 3 11 13 16 18 19 22 26 29 30 34 40 43 46 48 49 54 59 60 63 68 71 75 76 77 84 87 88 90 93 95 98 99 105 109 112 113	157
MFO	39	1 2 4 11 12 14 16 18 19 20 26 30 34 39 44 46 49 50 54 57 61 65 67 71 74 77 84 85 88 89 93 94 96 97 102 103 104 109 111	153
CS	37	1 6 9 10 13 16 18 19 20 26 29 30 38 41 44 47 54 57 59 63 67 71 76 80 82 85 90 93 95 99 100 103 104 106 107 109 111	168
WDO	45	2 4 5 7 12 16 17 18 20 26 29 34 36 37 41 42 45 49 50 54 55 57 59 63 64 68 71 74 78 79 80 81 82 89 92 93 94 95 96 100 102 103 105 109 111	185

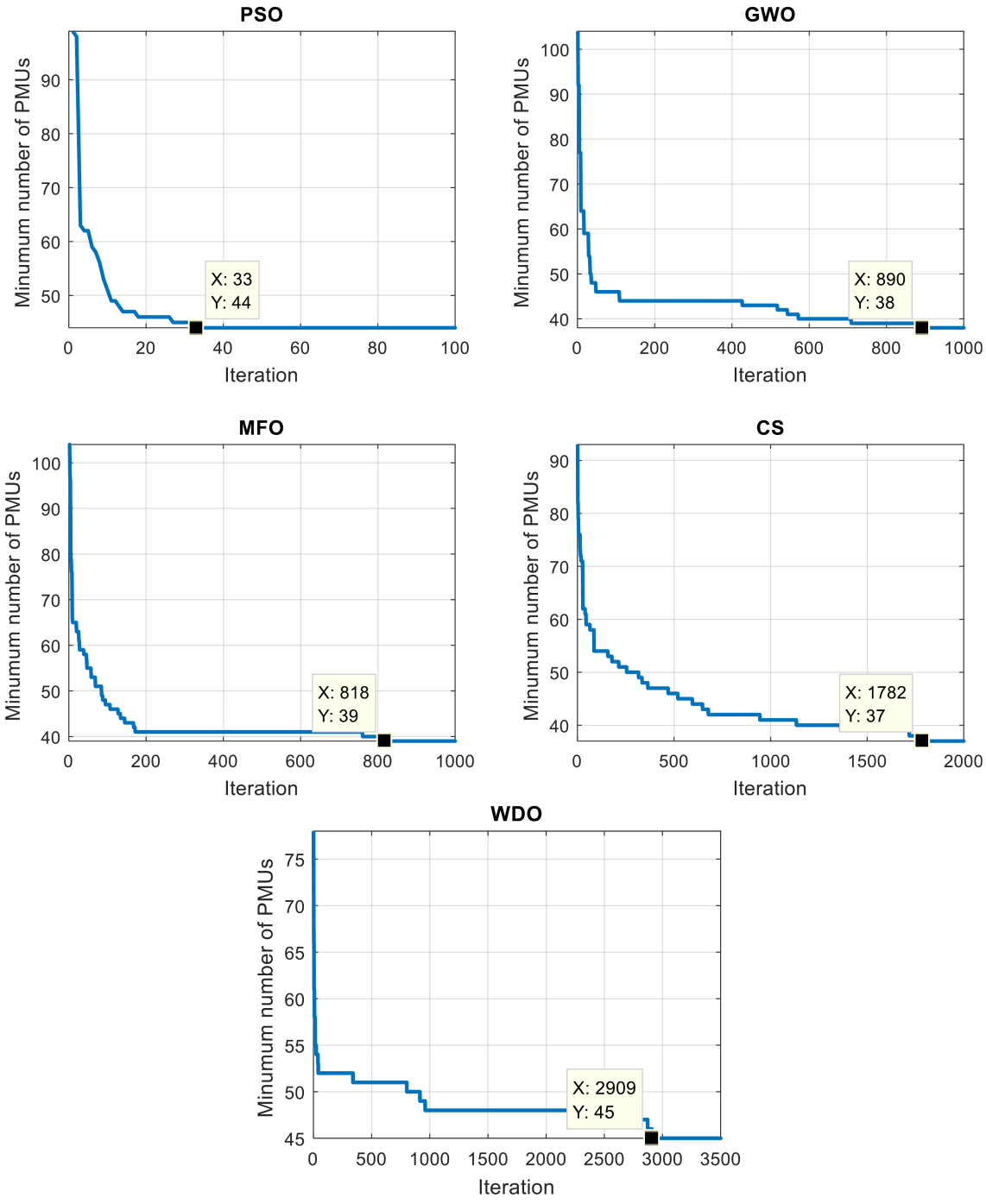

Figure 4.7. *The objective function graphs for the OPP problem of the Algerian grid system when ignoring ZIBs*

According to the results shown in Table 4.12, it is obvious that as the system complexity increases, the different applied algorithms do not converge to the same minimum number of PMUs due to the capability of each optimization method in solving this problem, for instance the WDO converges to 45 while the CS converges to 37, difference of 8 PMUs between the

aforementioned two algorithms and this considered to be a great difference in terms of cost. The same thing for the PSO algorithm that converges to 44. Whereas, the WDO and PSO algorithms cannot follow the complexity of the problem as the other three algorithms. Note that the number of PMUs achieved by the CS algorithm is smaller than what is obtained by GWO and MFO algorithms but it has a high value of SORI compared to GWO and MFO algorithms. Thus, the solution provided by the CS algorithm can be considered to be the appropriate solution.

For the case of PSO algorithm on IEEE 09-, 14-, 30-bus systems, this technique has been tested and validated successfully. However, for more complex system as the Algeria grid system, the limitation of this algorithm will be obvious, a similar remark is mentioned in [51]. That's why an improved PSO techniques has been established like the improved particle swarm optimization (IPSO) that is described in [52]. In IPSO, the features of Genetic Algorithm and Simulated Annealing are incorporated into PSO to overcome the PSO limitations.

It can be noticed in Figure 4.7 that the algorithm which can converge firstly to its final value is the PSO through the 33th iteration, where the worst one is the WDO algorithm which reaches its final value at 2909th iteration. Both of the two previously mentioned algorithms do not achieve a good results as the other algorithms. Thus, the way of how the algorithms converge to their final values has no effect in the quality of results.

4.3.4.2 Case of considering ZIBs

In this case, the presence of zero injection buses will be taken into consideration when the proposed algorithms are applied to solve the optimal phasor measurement unit placement problem (OPPP). As it is mentioned previously the Algerian network system has a twenty two (22) zero injection buses. The location of each zero injection bus is presented in Table 4.11.

As in the previous cases, the implemented program for each optimization method is executed with a population of particles equals to 200, and a high number of iterations to ensure that each algorithm will reach its possible best solution.

For each algorithm, the achieved minimum number of phasor measurement units required for the Algerian network system to be fully observable are presented in Table 4.13 in addition to the exact locations where the PMUs should be installed and the corresponding SORI value for each PMUs placement set. Also, the objective function graphs, which show the way how the algorithms converge to their final values, are depicted in Figure 4.8.

Table 4.13. *Optimal PMUs placement results for the Algerian grid system when considering ZIBs*

Methods	Number of PMUs	Positions	SORI
PSO	42	1 6 8 9 10 12 15 18 19 20 23 24 38 39 40 41 44 47 54 57 60 61 64 65 66 67 70 71 72 75 76 82 86 88 93 96 100 102 103 105 109 111	172
GWO	35	1 3 10 13 15 18 20 23 26 29 34 41 44 47 54 57 59 63 68 69 74 78 79 80 81 82 90 93 96 98 101 105 108 111 112	155
MFO	36	1 2 4 11 13 15 18 19 20 25 30 38 41 46 50 51 54 61 65 67 71 74 77 80 82 85 90 93 96 100 101 103 105 108 112 113	146
CS	34	4 6 13 15 18 19 20 24 34 36 40 42 46 49 53 55 57 59 63 68 69 74 80 82 87 90 93 96 97 102 105 109 111 112	142
WDO	49	4 5 6 7 8 11 12 13 16 19 22 25 29 33 34 36 41 43 44 47 52 56 61 62 65 67 71 72 73 74 77 84 85 86 87 88 89 90 92 96 97 98 100 101 103 104 109 112 113	190

Starting by the WDO algorithm, the achieved minimum number of PMUs is the same as when the ZIBs are ignored. Hence no reduction has been acquired.

In case of the PSO, the obtained result is 42 PMUs, even if there is a reduction of 2 PMUs, it is still having a bad result compared to the other three remaining algorithm results. Again, the WDO and PSO algorithms cannot follow the complexity of the problem as the other algorithms.

The required numbers of PMUs achieved by the algorithms MFO, GWO and CS are 36, 35 and 34 respectively, where a reduction of 3 PMUs is occurred compared to the case when the ZIBs are ignored. Therefore, the appropriate solution for the Algerian network system in the case of considering ZIBs is the solution provided by CS algorithms corresponding to minimum number of PMUs equals to 34.

As a confirmation for what has been mentioned in the previous section, Figure 4.8 shows that the PSO algorithm converges to its final value firstly while the WDO algorithm is the last

one. Both of the algorithms provide the worst results. Therefore, the way how the algorithms converge to their final value has no effect on results quality.

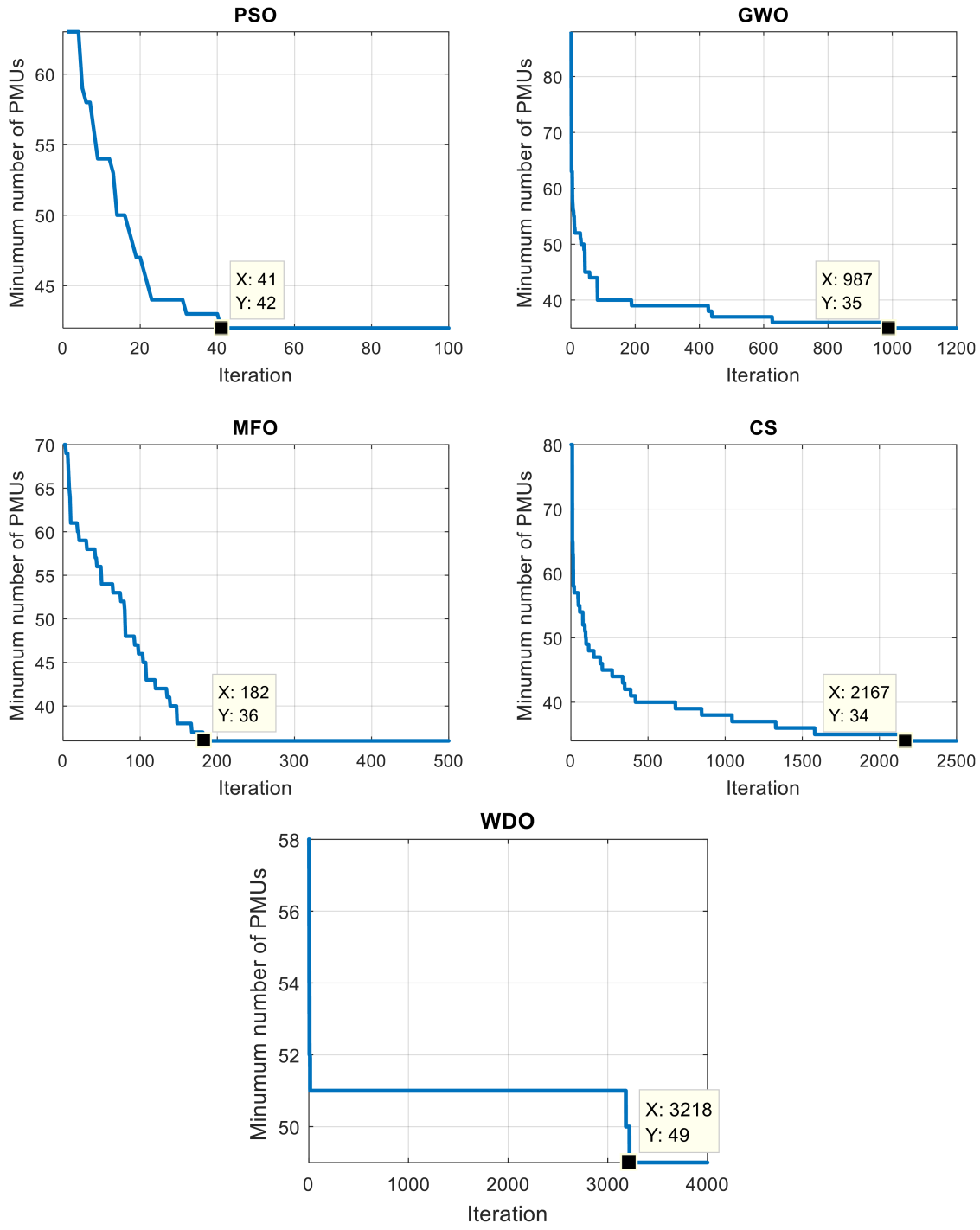

Figure 4.8. *The objective function graphs for the OPP problem of the Algerian grid system when considering ZIBs*

4.4 Conclusion

In this chapter all the proposed optimization algorithms presented in chapter 3, have been applied for solving the OPP problem that minimizes the number of PMUs and improves the observability redundancy of the power system. These algorithms have been applied on IEEE 09-bus, IEEE 14-bus, IEEE 30-bus and Algerian network systems, then the results have been compared with other methods reported earlier within the works performed by other researchers using other optimisation algorithms.

To sum up, it can be concluded that the number of PMUs required for ensuring the full observability of the studied power system increases as the power system size increases. Furthermore under such case, the all used algorithms cannot solve the OPPP when the dimension of the power system increases and this can be as a major drawback of using such algorithms.

General Conclusion

In this report, the optimal PMUs placement (OPP) that can ensure the full observability of the power system is investigated based on two practical cases such as ignoring and considering zero injection busses. Solving of the OPP problem has been performed based on the selected optimization methods, which are population-based methods using the natural intelligence of the swarm to determine the best solution. However, when dealing with large problem size, Population-based methods are widely known to tend to have performance problems such as the stagnation at local optima, instead of global optima that provides the optimal solution among the possible solutions. Recently, studies in this area have shown that the balance between exploitation and exploration must be maintained in order to prevent the search agents from being stuck in local optima.

For validation purposes, the selected methods are applied using MATLAB software to the IEEE 09-bus, 14-bus, 30-bus and Algerian 114-bus systems under the both cases of considering normal operation and ZIBs. The obtained results show that the different used algorithms converge to the same optima in simple systems, but the difference is reside in the way of how each algorithm can ensure the convergence to the optimal value. However, as the studied power system is more complex, the proposed algorithms converge to different values, this can be explained by the capability of the optimization method in finding the best solution or their premature convergences. In addition, it was found that the number of obtained PMUs is reduced when considering the ZIBs in the OPP.

The system observability redundancy index (SORI) that indicates the reliability of the PMUs placement set is used to distinguish among the different solutions in terms of reliability since there is no unique solution.

The following points describes the perspective works concerning the OPP problem:

- The application of the proposed methods in solving the OPP problem can be extended by taking different cases into consideration such as single PMU loss, PMU's channels limit and existing of conventional measurement devices.
- Implementing multi-objective optimization problem by taking the maximization of the system observability index (SORI) as second objective function.
- Applying the recently new optimization algorithms in the OPP problem.
- Developing a proper stop criterion of the optimization algorithm that can determine whether the current solution cannot be improved any more to avoid waste of computational costs.

References

[1] **H. Bentarzi,**“ Improving Monitoring, Control and Protection of PowerGrid Using Wide Area Synchro-Phasor Measurements (Presented as plenary lecture),” in Proc. 12th WSEAS Int. Conf. on Automatic control, modelling and simulation, Catania, Italy, ISSN: 1790-5117,ISBN:978-954-92600-1-4,PP.93-98, May 29-31, 2010.

[2] Jamuna.K, Yugin L Selva, Gnanasekaran , “Placement of PMUs for Power System Observability using Biogeography Based Optimization”, Third International Conference on Advances in Computing and Communications 2013.

[3] M. Shahriar, I. Habiballah and H. Hussein, "Optimization of Phasor Measurement Unit (PMU) Placement in Supervisory Control and Data Acquisition (SCADA)-Based Power System for Better State-Estimation Performance", Energies, vol. 11, no. 3, p. 570, 2018.

[4] IEEE Standard for Synchrophasor Measurements for Power Systems," in IEEE Std C37.118.1-2011 (Revision of IEEE Std C37.118-2005) , vol., no., pp.1-61, 28 Dec. 2011.

[5] M. Shafiullah, M. Abido, M. Hossain and A. Mantawy, "An Improved OPP Problem Formulation for Distribution Grid Observability", Energies, vol. 11, no. 11, p. 3069, 2018.

[6] G. Phadke, M. Ibrahim, T. Hlibka, "Fundamental Basis for Distance Relaying with Symmetrical Components", IEEE Trans. on PAS, Vol. PAS-96, No. 2, pp. 635-646, 1977.

[7] A. G. Phadke and J. S. Thorp, "HISTORY AND APPLICATIONS OF PHASOR MEASUREMENTS," 2006 IEEE PES Power Systems Conference and Exposition, Atlanta, GA, pp. 331-335, 2006.

[8] "USNO NAVSTAR Global Positioning System". U.S. Naval Observatory. [online]. http://tycho.usno.navy.mil/gpsinfo.html. Retrieved 2019-03-22.

[9] A. PHADKE and T. BI, "Phasor measurement units, WAMS, and their applications in protection and control of power systems", Journal of Modern Power Systems and Clean Energy, vol. 6, no. 4, pp. 619-629, 2018.

[10] D. Allan, N. Ashby, C. Hodge, “The Science of Timekeeping”, Hewlett Packard Application Note 1289, 1997.

[11] A. Phadke and J. Thorp, Synchronized phasor measurements and their applications. New York, NY: Springer, 2008.

[12] A. Monti, C. Muscas and F. Ponci, Phasor measurement units and wide area monitoring systems. Amsterdam: Academic Press is an imprint of Elsevier, 2016.

[13] R. F. Nuqui. State estimation and voltage security monitoring using synchronized phasor measurements. Doctor of Philosophy Dissertation, Virginia Polytechnic Institute and State University. July 2, 2001.

[14] A. MIRON, S. MIRON,C E. BOBRIC, C. POPA, L. PIERRAT, M. VIZITEU, “From scada to smart grid in power transmission and distribution systems”, Buletinul AGIR nr. 4/2011,octombrie-decembrie

[15] A.G. Phadke, J. S. Thorp, 2 chapters for "ADVANCES IN ELECTRIC POWER AND ENERGY CONVERSION SYSTEM DYNAMICS AND CONTROL", edited by C. T. Leondes

[16] **A. Ouadi, H. Bentarzi** and J. C. Maun, "A new computer based Phasor Measurement Unit framework," 2009 6th International Multi-Conference on Systems, Signals and Devices, Djerba, pp. 1-6, 2009.

[17] L. Hua, D. Yi, S. Sandeep, J.S. Thorp, M. Lamine. “Cyber Security Impacts on All-PMU State Estimator – A Case Study on Co-Simulation Platform GECO” (2012).

[18] Andrew Armenia, Joe H. Chow, “A Flexible Phasor Data Concentrator Design Leveraging Existing Software Technologies”, IEEE Transactions On Smart Grid, June 2010.

[19] Zhenyu Huang, Bogdan Kasztenny, Vahid Madani, and other, “Performance Evaluation of Phasor Measurement” IEEE Power Engineering Society General Meeting 2008, Pittsburgh, PA.

[20] A. P. Sakis Meliopoulos, G. J. Cokkinides, F. Galvan and B. Fardanesh, "GPS-Synchronized Data Acquisition: Technology Assessment and Research Issues," Proceedings of the 39th Annual Hawaii International Conference on System Sciences (HICSS'06), Kauia, HI, USA, pp. 244c-244c, 2006.

[21] IEEE Standard for Synchrophasors for Power Systems," in IEEE Std C37.118-2005 (Revision of IEEE Std 1344-1995) , vol., no., pp.0_1-57, 2006

[22] IEEE/IEC International Standard - Measuring relays and protection equipment - Part 118-1: Synchrophasor for power systems - Measurements," in IEC/IEEE 60255-118-1:2018 , vol., no., pp.1-78, 19 Dec. 2018

[23] Mohammad Shahraeini and Mohammad Hossein Javidi. Wide Area Measurement Systems, Advanced Topics in Measurements, Md. Zahurul Haq, Intech Open, 2012.

[24] **H. Bentarzi**, M. Tsebia and A. Abdelmoumene, "PMU based SCADA enhancement in smart power grid," 2018 IEEE 12th International Conference on Compatibility, Power Electronics and Power Engineering (CPE-POWERENG 2018), Doha, pp. 1-6, 2018.

[25] Schweppe FC, Wildes J, Rom DB. Power system static-state estimation, part I, II and III. IEEE Trans Power Syst;89(1):120–35, 1970.

[26] A. Abur and A. Gómez Expósito, Power system state estimation. New York: Marcel Dekker, 2004.

[27] Johnson A., R Bravo, & S. Robles, "Operating the Grid Better with Phasor Data -- Understanding FIDVR," presented to the NERC Operating Committee, December 2010.

[28] White, A. & S. Chisholm, June 2011, “SynchroPhasor Use at OG&E," presented to the NERC Operating Committee

[29] A. G. Phadke, J. S. Thorp, and K. J. Karimi, “State Estimation with Phasor Measurements”, in IEEE Transactions on Power Systems, Vol. 1, No. 1, pp. 233-241, February 1986.

[30] G. R. Krumpholz, K. A. Clements and P. W. Davis, "Power System Observability: A Practical Algorithm Using Network Topology," in *IEEE Transactions on Power Apparatus and Systems*, vol. PAS-99, no. 4, pp. 1534-1542, July 1980.

[31] H. Mori and S. Tsuzuki, "A fast method for topological observability analysis using a minimum spanning tree technique", IEEE Transactions on Power Systems, vol. 6, no. 2, pp. 491-500, 1991.

[32] T. L. Baldwin, L. Mili, M. B. Boisen, and R. Adapa, “Power System Observability with Minimal Phasor Measurement Placement”, IEEE Trans. on Power Systems, Vol.8, No. 2, pp. 701-715, 1993.

[33] K. A. Clements and B. F. Wollenberg, “An algorithm for observability determination in power system state determination,” in IEEE Power Eng. Soc. Summer Meeting, San Francisco, CA, Paper A 75 447-3, 1975.

[34] A. Enshaee, R. A. Hooshmand, and F. H. Fesharaki, “A new method for optimal placement of phasor measurement units to maintain full network observability under various contingencies,” Electric Power Systems Research, vol. 89, pp. 1–10, 2012.

[35] D. Dua, S. Dambhare, R. K. Gajbhiye, and S. A. Soman, “Optimal multistage scheduling of PMU placement: An ILP approach,” IEEE Trans. Power Deliv., vol.23, no. 4, pp. 1812–1820, 2008.

[36] J. Kennedy and R. Eberhart, "Particle swarm optimization," in Neural Networks, 1995. Proceedings., IEEE International Conference on, pp. 1942-1948, 1995.

[37] **A.L. Kouzou** and R.D Mohammedi**,** "Selective Harmonic Elimination PWM For A Multi-level Inverter Based On Particle Swarm Optimization", The second International Conference on Applied Automation and Industrial Diagnostics ICAAID, Algeria, 2017.

[38] S. Mirjalili, S. Mirjalili and A. Lewis, "Grey Wolf Optimizer", Advances in Engineering Software, vol. 69, pp. 46-61, 2014.

[39] S. Mirjalili, "Moth-flame optimization algorithm: A novel nature-inspired heuristic paradigm", *Knowledge-Based Systems*, vol. 89, pp. 228-249, 2015.

[40] K. Gaston, J. Bennie, T. Davies and J. Hopkins, "The ecological impacts of nighttime light pollution: a mechanistic appraisal", *Biological Reviews*, vol. 88, no. 4, pp. 912-927, 2013.

[41] K.D. Frank, C. Rich, T. Longcore, ”Effects of artificial night lighting on moths”, Journal of Ecological consequences of artificial night lighting, Hindawi Publishing Corporation, Vol. 2015, No. 1, pp. 305-344, 2006.

[42] X. Yang and Suash Deb, "Cuckoo Search via Lévy flights," 2009 World Congress on Nature & Biologically Inspired Computing (NaBIC), Coimbatore, 2009, pp. 210-214.

[43] X.-S. Yang, Nature-inspired metaheuristic algorithms. Frome, U.K.: Luniver Press, 2010.

[44] Z. Bayraktar, M. Komurcu, and D. H. Werner, “Wind Driven Optimization (WDO): a novel nature-inspired optimization algorithm and its application to electromagnetics,” in Proceedings of the Antennas and Propagation Society International Symposium (APSURSI), pp. 1–4, IEEE, Toronto, Canada, July 2010.

[45] Z. Bayraktar, M. Komurcu, J. Bossard and D. Werner, "The Wind Driven Optimization Technique and its Application in Electromagnetics", *IEEE Transactions on Antennas and Propagation*, vol. 61, no. 5, pp. 2745-2757, 2013.

[46] J. Wallace and P. Hobbs, *Atmospheric science an introductory survey*. Canada: Elsevier, 2005.

[47] K. Joe Cherian and S. Smitha, "Optimum placement of PMU for wide area protection", International Journal of Innovative Research In Technology, vol. 3, no. 3, pp. 215 - 218, 2016.

[48] S. Singh and S. Singh, "A Multi-objective PMU Placement Method in Power System via Binary Gravitational Search Algorithm", Electric Power Components and Systems, vol. 45, no. 16, pp. 1832-1845, 2017.

[49] "pg_tca30bus", Labs.ece.uw.edu, 2019. [online]. Available: http://labs.ece.uw.edu/pstca/pf30/pg_tca30bus.htm. Retrieved 17-04- 2019.

[50] Y. Amrane, A. Elmaouhab, M. Boudour and A. Ladjici, "Voltage stability analysis based on multi - objective optimal reactive power dispatch under various contingency", International Journal on Electrical Engineering and Informatics, vol. 9, no. 3, pp. 521-541, 2017.

[51] M. Sefid and M. Rihan, "Optimal PMU placement in a smart grid: An updated review", International Journal of Smart Grid and Clean Energy, vol. 8, no. 1, pp. 59-69, 2019.

[52] Wang J, Li C, Zhang J. Optimal Phasor Measurement Unit Placement by an Improved PSO Algorithm. In: Proc. of 2012 Asia-Pacific Power and Energy Engineering Conference, pp. 1–4, 2012.

Appendix A.1

The Pseudo code of PSO algorithm

for *each particle*
    Initialize particle
end
do
   for *each particle*
        Calculate fitness value
       if *the fitness value is better than the best fitness value in history*
         set current values as new best fitness values
       end if
   end for
   Choose the particle with the best fitness value of all the particles as the X_g*best*
   for *each particle*
        Calculate particle velocity according equation (3.8)
       Update particle position according equation (3.7)
   end for
while *maximum iterations or minimum error criteria is not attained*

The Pseudo code of GWO algorithm

Initialize the grey wolf population $\overrightarrow{X_{wolf}}$ *(i = 1, 2, ..., n)*
Initialize a, A, and C
Calculate the fitness of each search agent
X_α*=the best search agent*
X_β*=the second best search agent*
X_δ*=the third best search agent*
while *(t < Max number of iterations)*
       for *each search agent*
            Update the position of the current search agent by equation (3.15)
     end for
    Update a, A, and C
    Calculate the fitness of all search agents
    UpdateX_α, X_β, *and* X_c
     t=t+1
end while
return X_α

Appendix A.2

The Pseudo code of MFO algorithm

Initialize a population of n flames positions randomly in the search space.
while *(maximum number of iteration not reached)*
Update the number of flames (N_{flames}) to be used according to equation (3.19).
Calculate the fitness of all the n moths.
if *first iteration then*
Sort the moths from best to worst according to their fitness and place the result in flame matrix.
else
Merge the population of past moths and flames. Sort the merged population from best to worst.
Select the best N positions from the sorted merged population as the flames.
end if
Calculate the convergence constant r.
for *each Moth i with* $i \leq n$ *do*
Calculate t as $t = (r - 1) * rand + 1$.
if $i \leq N$ *then*
Update Moth i position according to Flame i using equation (3.18).
else
Update Moth i position according to Flame ($i=N_{flames}$) *using equation (3.18).*
end if
end for
end while

The Pseudo code of CS algorithm

Objective function f(x); $x = (x_1,.., x_d)$
Generate initial population of n host nests x_i
while *(t <MaxGeneration) or (stop criterion)*
Get a cuckoo randomly,generate a solution by lévy flight and then evaluate its quality fitness Fi.Choose a nest among n (say, j) randomly
if *(Fi > Fj),*
Replace j by the new solution
end
A fraction ($1-P_a$) *of worse nests are abandoned and new ones/solutions are built/generated*
Keep best solutions (or nests with quality solutions) Rank the solutions and find the current best
end while

Appendix A.3

The Pseudo code of WDO algorithm

Generate initial population of n air parcels (positions and its velocities)
Evaluate the pressure (fitness) value for each air parcels
Sort the population from best to worst to associate each air parcel with its rank (i)
Find the best particle in population (X_{opt})
while *(t <MaxGeneration) or (stop criterion)*
    Update air parcel velocities according to equations (3.37) and (3.39)
    Update air parcel positions according to equation (3.38)
    Evaluate population pressure (fitness) value
    Sort the population from best to worst to associate each air parcel with its rank (i)
    Find the best particle in population (X_{opt})
end while
return X_{opt}

Appendix B

IEEE 09-bus system data

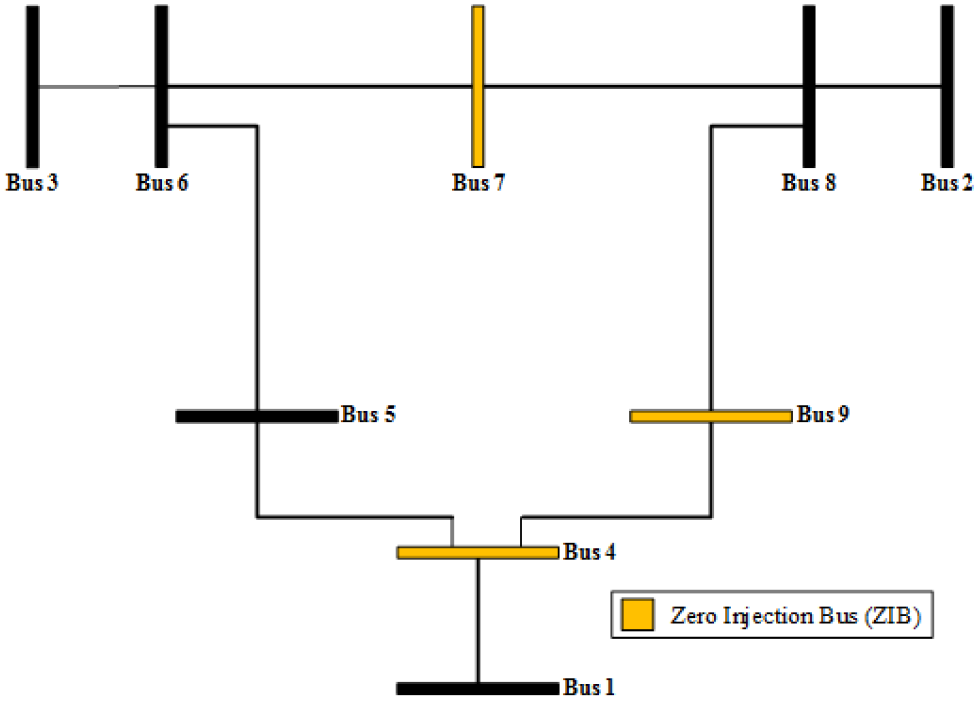

Branches	
From bus	**To bus**
1	4
2	7
3	9
4	5
4	6
5	7
6	9
7	8
8	9

Appendix C

IEEE 14-bus system data

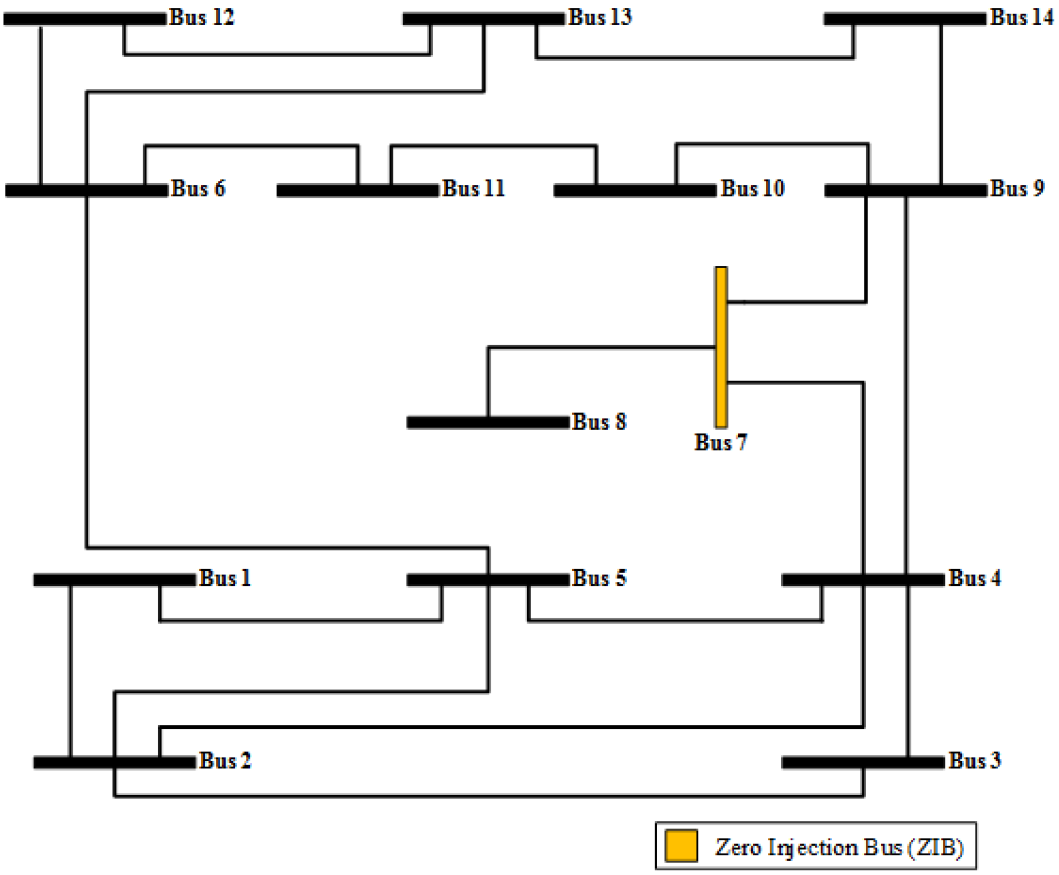

Branches		Branches	
From bus	**To bus**	**From bus**	**To bus**
1	2	6	11
1	5	6	12
2	3	6	13
2	4	7	8
2	5	7	9
3	4	9	10
4	5	9	14
4	7	10	11
4	9	12	13
5	6	13	14

Appendix D

IEEE 30-bus system data

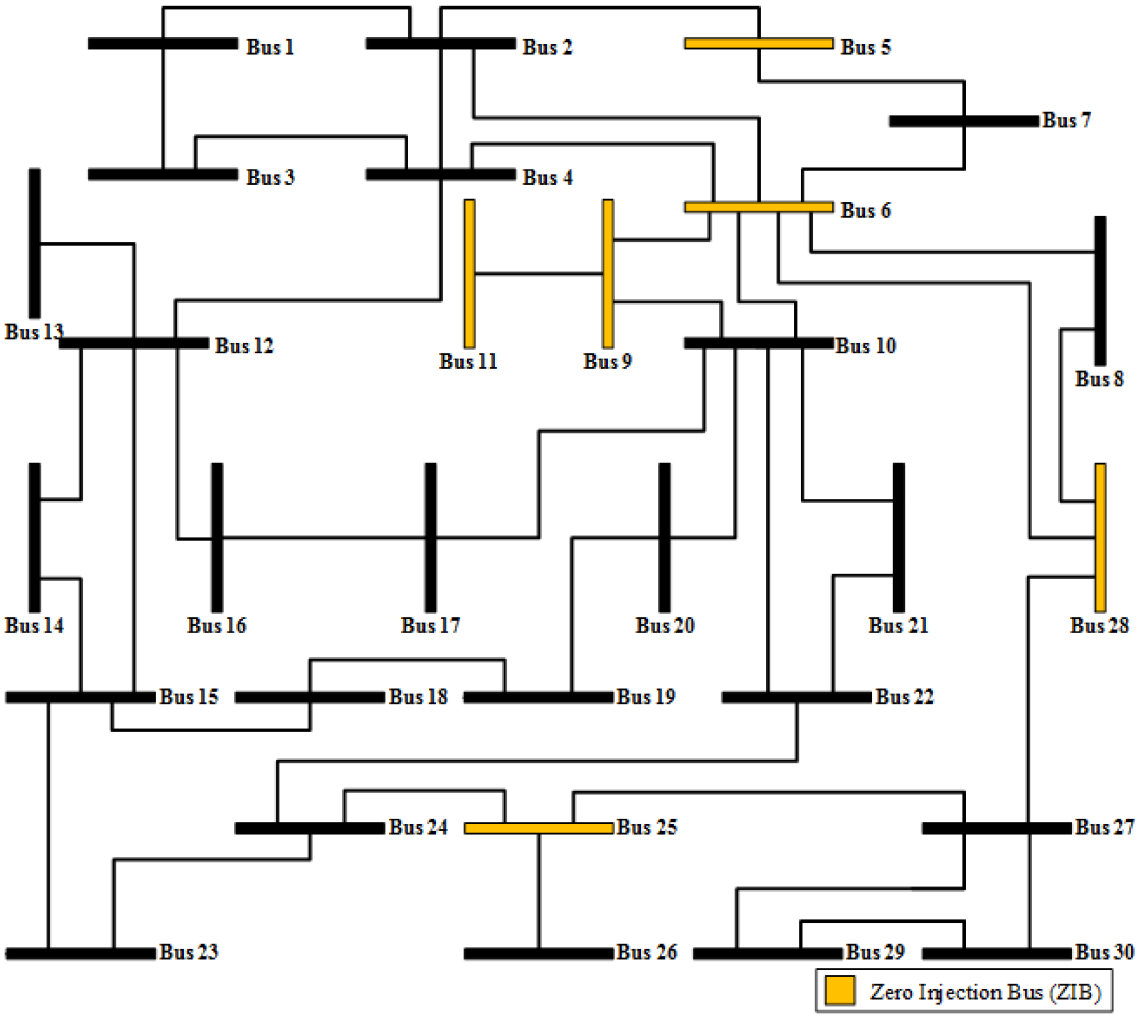

Branches		Branches		Branches	
From bus	To bus	From bus	To bus	From bus	To bus
1	2	8	28	16	17
1	3	9	10	18	19
2	4	9	11	19	20
2	5	10	17	21	22
2	6	10	20	22	24
3	4	10	21	23	24
4	6	10	22	24	25
4	12	12	13	25	26
5	7	12	14	25	27
6	7	12	15	27	28
6	8	12	16	27	29
6	9	14	15	27	30
6	10	15	18	29	30
6	28	15	23		

Appendix E

Algerian 114-bus system data (2011)

Branches		Branches		Branches		Branches	
From bus	To bus	From bus	To bus	From bus	To bus	From bus	To bus
1	4	20	24	45	46	81	86
1	5	20	29	46	47	81	90
1	7	20	32	47	48	82	83
1	8	20	35	47	50	82	87
1	42	20	52	51	57	82	94
1	42	20	52	52	53	83	84
2	3	21	44	52	59	84	100
2	6	21	60	53	54	85	86
3	6	22	24	54	55	85	87
3	9	22	24	54	56	86	93
4	5	22	32	54	59	87	99
4	6	22	37	56	57	87	100
4	9	23	30	56	57	87	106
4	16	23	36	57	58	89	90
6	7	24	25	57	77	89	90
7	10	25	26	58	72	90	93
8	42	26	27	58	75	91	93
10	11	26	28	59	60	91	93
10	13	26	29	59	61	92	93
11	42	26	29	62	73	94	98
12	13	26	34	63	64	95	96
14	16	28	31	63	65	96	98
15	16	29	35	63	65	97	98
17	18	29	39	63	66	97	100
17	20	30	31	64	97	98	99
17	21	30	36	66	67	98	100
17	27	30	52	66	73	99	100
17	31	31	60	67	68	99	101
17	72	32	33	67	73	99	102
17	64	34	38	68	70	101	102
18	20	40	41	69	71	101	105
18	22	40	50	70	71	101	107
18	33	41	42	71	72	103	105
18	37	41	49	72	96	103	106
18	62	42	44	72	101	103	110
18	73	42	44	74	75	103	114
18	73	42	48	74	76	104	105
19	26	43	44	75	107	107	109
19	26	43	51	80	82	108	109
19	34	43	55	80	84	110	112
19	78	44	45	80	84	111	112
19	79	44	48	80	88	111	113
20	21	44	58	81	82	112	114
20	24	44	60	81	85		